The cow udder is a potential mixing vessel for influenza A viruses

Authors

Rute Maria Pinto[1!*], Colin P Sharp[1*], Maia Beeson[1], Nunticha Pankaew[1], Jack A. Hassard[2], Alexander Moxom[1], Callum Magill[3], Laura Tuck[1], Stephen Meek[1], Hui Min Lee[1], Kirsty Jensen[1], Inga Dry[1], Pedro Melo[1], Jiayun Yang[4], Ashwin Ashok Raut[5], Anamika Mishra[5], Sjaak de Wit[6,7], J. Ross Fitzgerald[1], Jayne C. Hope[1], Joanne Stevens[1], Tom Burdon[1], Kate Sutton[1], Cristina L. Esteves[1], F. Xavier Donadeu[1], Ian Brown[4], Wendy Barclay[8], Thomas P. Peacock[4] Daniel H. Goldhill[9], Munir Iqbal[4], Pablo R. Murcia[3], Stuart M. Haslam[2], Eleanor Gaunt[1!], Paul Digard[1!]

[1]The Roslin Institute, The University of Edinburgh, Easter Bush Campus, Midlothian EH25 9RG, UK

[2]Department of Life Sciences, Imperial College London, London, SW7 2AZ, UK

[3]MRC-University of Glasgow Centre for Virus Research, Garscube Campus, 464 Bearsden Road, Glasgow G61 1QH , UK

[4]The Pirbright Institute, Ash Road, Pirbright, Woking, GU24 0NF, UK

[5]Indian Council of Agricultural Research-National Institute of High Security Animal Diseases, Bhopal, MP, India- 462022

[6]Royal GD, Deventer, the Netherlands

[7]Veterinary Faculty, Utrecht University, Utrecht, the Netherlands

[8]Department of Infectious Disease, Imperial College London, London, UK

[9]The Royal Veterinary College, Hawkshead Lane, North Mimms, Hatfield, Hertfordshire, AL9 7TA, UK

[*]equal contribution

[!]co-corresponding

Abstract

The incursion of high pathogenicity avian influenza A virus (IAV) into US dairy cows is unprecedented in the era of molecular diagnosis and pathogen sequencing. This raises questions over the likelihood of further outbreaks and whether dairy cattle could be a mixing vessel for novel strains of IAV. Using a panel of BSL2-safe reassortant viruses representing clade 2.3.4.4b H5 epizootic lineages circulating since 2020, we found that a cow B3.13 isolate displayed enhanced replication in cow mammary gland cells, along with increased viral polymerase activity and stronger interferon antagonism in cow cells compared to an earlier EA-2020-C genotype virus. However, multiple avian and mammalian IAV strains, including other clade 2.3.4.4b high pathogenicity genotypes, were replication competent in bovine cells, particularly those of the mammary gland, suggesting that there is a diverse circulating IAV pool with the potential to infect cows. Moreover, we show that cow mammary cells co-express α-2,3 and α-2,6 – linked sialic acids, and are susceptible to co-infection with human and avian IAVs. We conclude that the US cow influenza outbreak does not simply reflect a unique adaptation of the B3.13 genotype virus; rather, the bovine udder represents a permissive niche for IAV and a plausible site for reassortment, underscoring its potential role in generating novel influenza viruses with pandemic risk.

212 words

Introduction

Since 2020, the H5N1 clade 2.3.4.4b of influenza A virus (IAV) has spread globally, threatening diverse wild bird species and causing economic devastation to the poultry industry. This panzootic has also resulted in multiple intra-phylum spill-over events, including farmed mink, semi-aquatic mammals and, in 2024, dairy cows [1, 2]). Since the detection of the B3.13 genotype H5N1 in cattle in March 2024, it has demonstrated sustained, widespread inter-state transmission in dairy cattle [3, 4]. This was unexpected, as until this event, fully verified evidence of IAV infection in cows has been limited, especially with regards to sequenced virus isolates available for further study [5]. While IAV is generally respiratory-tropic in mammals, the primary clinical indicator in the current bovine outbreak is an abrupt drop in milk production [6], correlating with high viral loads in milk [2]. Initial evolutionary and molecular analyses of cattle B3.13 viruses suggested that these viruses had quickly acquired mammalian associated adaptations in several genes [7]. Isolates were replication competent in human cell lines, were highly pathogenic in mice and ferrets [8, 9] and concomitantly, there have been multiple independent reports of zoonotic infections in dairy farm workers [10-12]. These events raised important questions around the likelihood of further IAV incursions into cattle and the pandemic potential of such outbreaks. We show here that a range of cow-derived cells are susceptible to infection with various IAV strains of avian, human or swine origin, that primary cow mammary cells express both α-2,3 and α-2,6 N-acetylneuraminic acid and that these cells can be co-infected with human and avian IAVs. We conclude that other IAV strains have the potential to infect cows and that this could yield reassortant viruses with zoonotic and pandemic potential.

Results

Cow mammary epithelial cells are susceptible to infection with diverse IAV strains.

While IAV is traditionally considered to be a respiratory virus in mammalian species, transmission of B3.13 viruses between dairy cows has been associated with the use of milking

equipment [13]. We therefore asked whether cow mammary gland epithelial cells are more susceptible to IAV infection than other cell types. Cow primary and immortalised cells originating from different anatomical sites (Figure 1A) were infected with a variety of IAV strains representative of four categories: laboratory-adapted, human, swine and avian. Infections were performed at low multiplicity of infection (MOI) and viral growth kinetic analyses were conducted up to 48 hours post infection (hpi). Of all tested cells, mammary cells showed the highest susceptibility to infection, with lab-adapted strains reaching viral titres of 10^{8} PFU/ml. Titres of $10^{6\text{-}7}$ PFU/ml were detected for viruses of human, swine and avian origins. Respiratory, anatomically diverse fibroblast, and immune cells were less permissive to IAV infection, with peak titres typically 2 to 3 orders of magnitude lower than those achieved in mammary cells across all virus strains (Figure 1B, Supplementary Figures S1-3). This further correlates with the ability of cow mammary cells to support the polymerase activity of diverse IAV strains (Figure 1C). The tropism of B3.13 for mammary gland epithelial cells therefore appears to be a generalisable phenomenon, observed across diverse IAV strains isolated from hosts spanning multiple taxonomic classes.

B3.13 internal gene constellation confers better virus replication in cow cells.

The inherent permissiveness of cow mammary cells to IAV infection does not explain why B3.13 was particularly successful at sustaining onward transmission in cows. We hypothesised that the unexpected dissemination of B3.13 infections in dairy cows could be explained by a fitness advantage of these viruses over other genotypes. To test this, biosafety level 2 viruses representative of an early B3.13 cow isolate ('Cattle Texas') and an avian precursor (AIV07, EURL genotype EA-2020-C) were generated harbouring the glycoproteins of the laboratory-adapted strain A/Puerto Rico/8/1934 H1N1 (PR8). These viruses were used to infect bovine cells from different tissues including mammary epithelial cells (bMEC), type II pneumocytes, skin and heart fibroblasts and blood-derived macrophages (BDϕ) as well as mammary gland explants and surface-grown intestinal organoid cultures (2D enteroids). With the exception of bMECs, where AIV07 replicated slightly better, Cattle Texas replicated to 10

102 to 10,000-fold higher titres compared to AIV07 (Figure 2). Therefore, Cattle Texas
103 demonstrated a fitness advantage in bovine cells compared to a representative avian virus
104 precursor.

105 After entering North America through the Atlantic bird migratory route, EA-2020-C
106 viruses like AIV07 reassorted with the local low pathogenic avian influenza (LPAI) pool, giving
107 rise to the B3.13 genotype via acquisition of new viral genome segments 1, 2, and 5 (encoding
108 the PB2, PB1 and NP components of the viral ribonucleoprotein (RNP) complex respectively),
109 [14] as well as segment 8 (encoding NS1 and NS2) [7, 15, 16] (Figure 3A). Therefore, we
110 investigated whether the new RNP segments improved viral transcription activity in cow cells
111 using a bovine-specific minigenome reporter assay [17]. Cattle Texas RNPs were 20-times
112 more efficient than AIV07 (Figure 3B, open blue and yellow bars). To determine which
113 segments contributed to this improved activity, Cattle Texas and AIV07 RNPs were
114 reconstituted with reciprocal single gene replacements, including segment 3 (encoding PA),
115 the final component of the viral polymerase. Replacing Cattle Texas PB1 with the AIV07
116 counterpart had no effect, while swapping NP increased RNP activity in MAC-T cells (Figure
117 3B, yellow cross-hatched bars). In contrast, PB2 or PA from AIV07 significantly decreased
118 Cattle Texas minireplicon activity. In the reciprocal swaps, AIV07 polymerase activity was
119 improved by up to 5-fold by Cattle Texas segments 1, 2 or 3, but replacement of segment 5
120 had an 8-fold negative impact on polymerase efficiency (Figure 3B, green cross-hatched bars).
121 Thus, the increased polymerase activity of Cattle Texas is attributable to the PB2- and PA-
122 encoding segments. To test this in a viral context, we made reassortant viruses in which Cattle
123 Texas PB2 or all polymerase segments were replaced with those of AIV07. Both PB2 and full
124 polymerase swap viruses exhibited reduced replication in cow mammary cells (Figure 3C),
125 confirming the importance of these segments.

126 NS1 is the primary IAV IFN antagonist, working through multiple partially redundant
127 but also strain-specific mechanisms, including both general repression of cellular gene
128 expression at transcriptional and translational levels as well as specific inhibition of IFN
129 induction [18]. As an initial test of whether reassortment of segment 8 was phenotypically

important, we assessed host cell shut off by infecting MAC-T cells with the PR8 6:2 Cattle Texas or a PR8 2:5:1 Cattle Texas harbouring AIV07 segment 8 and pulsed the cells with puromycin at various times post infection. Western blotting for the puromycin-labelled prematurely terminated polypeptides indicated that while both viruses repressed cellular translation at late times post infection, there was no major difference between them (Figure S4A). As a more quantitative measure of shut off, we co-transfected MAC-T cells with segment 8 plasmids from the two viruses alongside a constitutive expression plasmid encoding Renilla luciferase and measured the resulting luminescence. Both NS1 proteins showed dose-dependent inhibition in this assay with Cattle Texas showing a modest improvement over AIV07 (Figure S4B). The PA-X accessory gene expressed from segment 3 also contributes to IAV host cell shut off [14]. Although segment 3 reassortment did not occur between genotypes EA-2020-C and B3.13, genetic drift led to four amino acid differences between the PA-Xs of AIV07 and Cattle Texas, three of which lie within the “X-ORF” (Figure S4C). Therefore, we similarly compared the ability of AIV07 and Cattle Texas PA-X proteins to inhibit host gene expression, but no significant differences were observed (Figure S4D).

To test specific IFN antagonism by NS1, the AIV07 and Cattle Texas segment 8 plasmids were transfected into MAC-T cells alongside an IFN-β reporter plasmid and the cells stimulated with poly I:C as a mimic for viral RNA. This showed that, at similar expression levels, Cattle Texas NS1 had a significantly higher ability to counteract type I IFN induction than AIV07 NS1 (Figure 3D). To assess the contribution of this to overall virus fitness, replication of the 2:5:1 Cattle Texas reassortant virus harbouring AIV07 segment 8 was characterised in MAC-T and BAT-II cells. Introduction of AIV07 NS into Cattle Texas resulted in a slight but non-statistically significant delay in virus propagation in mammary epithelial cells, but had a much larger effect in the pneumocyte cell line (Figure 3E), suggesting that changes in segment 8 also contribute to the improved fitness of Cattle Texas over AIV07. Thus overall, the reassortment events that replaced segments 1, 2 and 8 alongside drift adaptations in segment 3 may have contributed to the ability of the B3.13 genotype virus to infect cattle.

158 Spill-back of the cattle B3.13 virus into poultry has been observed on multiple
159 occasions [3, 19], despite its evident fitness adaptations for bovines. The 2:6 Cattle Texas
160 virus replicated to slightly lower titres in chicken lung epithelial cells than AIV07, while its
161 polymerase and NS1 exhibited similar activities to those of the AIV07 proteins in the same
162 cells (Supplementary Figure S5). Thus the enhanced fitness of Cattle Texas in bovine cells is
163 specific to bovine cells but does not carry a high fitness penalty in chicken cells.
164

165 **Cow mammary cells are susceptible to European 2.3.4.4b genotype viruses and support**
166 **co-infection by human and avian viruses.**

167 Detections of IAV in US dairy cattle are mostly of North American H5N1 2.3.4.4b
168 genotypes B3.13 and, more recently, D1.1 viruses. Therefore, we asked whether similar dairy
169 cattle incursions could happen in countries where the B3.13 and D1.1 genotypes are not
170 circulating. To that end, we compared the growth kinetics of Cattle Texas with other avian
171 European 2.3.4.4b genotypes in primary and continuous bovine mammary cells and explants,
172 again all as 2:6 reassortants with PR8 glycoproteins to permit work at BSL2. In addition to
173 AIV07 (genotype EA-2020-C), these included a 2.3.4.4b 2020 H5N8 precursor (H5N8-20) and
174 EURL genotypes EA-2021-AB (AIV09) and EA-2022-BB (AIV48) (Figure 4A). In all three
175 systems, Cattle Texas replicated to the highest titres, perhaps as expected for a virus with
176 bovine-adapted internal segments, but other unadapted 2.3.4.4b strains (in particular BB
177 genotype AIV48) also replicated to high titres (Figure 4A). Cow mammary explants showed
178 the greatest range of virus titres, with H5N8-20 and AIV07 exhibiting very poor fitness in this
179 model, such that many of the explants were refractory to infection or only yielded low titres
180 (Figure S6). This suggests that recent Clade 2.3.4.4b H5N1 genotypes on both sides of the
181 North Atlantic have the potential to cause dairy cattle infections.

182 Human IAV pandemics classically arise from reassortment between avian and
183 mammalian strains [20, 21]. Historical data suggest the incursion of human seasonal strains
184 into cattle [5], so in the face of an ongoing H5N1 epidemic in birds and cattle, the possibility
185 of the cow udder as a “mixing vessel” arises. However, co-infection of a single cell harbouring

186 both avian and mammalian receptor types is needed for this mixing to occur. Lectin staining
187 analyses indicate the presence of α-2,3 linked sialic acid receptors for circulating avian H5
188 viruses in cow mammary glands [22-24], while our own infectivity data (Figures 1, S1) suggest
189 the presence of human α-2,6 linked sialic acids on bovine mammary epithelial cells. To
190 establish the amounts of each receptor type in the cells used here, we next performed
191 quantitative glycomic analyses on the immortalised and therefore likely relatively
192 homogeneous (MAC-T) and primary, potentially heterogeneous (bMEC) cell populations. This
193 identified complex N-glycans containing a mix of α-2,3 and α-2,6 linked sialic acids, with a
194 higher proportion of α-2,6 linkages present on the bMECs compared to MAC-T cells (Figure
195 4B, C; Supplementary Figures S7-S10). Cow mammary cells therefore express the sialic acids
196 required for infection with both avian and mammalian IAVs; however, this does not
197 demonstrate that the two sialic acid conformations are present at functionally relevant levels
198 on the same cell. To determine whether individual cow mammary gland cells could be co-
199 infected by human and avian strains of virus, bMEC cells were inoculated with an α-2,6 sialic
200 acid-dependent human seasonal H1N1 strain and an α-2,3 sialic acid-dependent low
201 pathogenicity avian virus, either singly or together. Infected cells were fixed and stained with
202 anti-H1 or H3 HA and analysed by flow cytometry. The individual infections confirmed antibody
203 specificity, while a dual-infected population was clearly visible in the co-infection sample
204 (Figure 4D). We therefore conclude that co-infections of human and avian viruses within the
205 cow mammary glands are possible, supporting the possibility of reassortment events.
206

207 **Discussion**

208 The unexpected influenza outbreak in US dairy cows requires careful consideration to
209 understand why it occurred, and its potential implications for both livestock and human health
210 [15]. At one extreme, it could have resulted from a rare adaptation of the B3.13 genotype to
211 allow infection of a species usually refractory to infection with most strains of IAV; at the other,
212 an unusually large and well documented epidemic of a not uncommon spillover event that

213 mostly goes undetected. To experimentally test these possibilities, we compiled a variety of
214 bovine cell culture systems and performed a systematic analysis of their susceptibility to IAV
215 infection. We found that while there are clear virus strain and cell-type differences in the
216 susceptibility of bovine cells to IAV infection, many cell types are susceptible to infection with
217 a diverse range of avian and mammal viruses. Notably however, mammary gland epithelial
218 cells are the most susceptible to infection compared to respiratory, immune or fibroblast cells,
219 consistent with the clinical manifestations of mastitis and high viral loads present in milk [4,
220 25].

221 The ability of cow mammary cells to be infected with and support high levels of
222 replication of a wide range of IAV strains here described argues against the extreme
223 hypothesis of a truly unique phenotypic trait of the B3.13 strain that permits infection of cows.
224 These observations are consistent with recent studies showing that other avian 2.3.4.4b
225 isolates are able to replicate in bovine cells [26-28] and udders [25, 29], as well as the more
226 recently detected D1.1 genotype spillover into US dairy cattle [30]. However, our findings of
227 wide variation in the ability of specific strains of IAV to replicate in bovine cells suggests that
228 adaptation does play a role. Thus, we sought to determine what, if anything, predicted the
229 emergence and transmission of Cattle Texas above other avian IAV strains. We found a
230 multifactorial scenario, with improvements in polymerase efficiency and the ability of NS1 to
231 counteract type I interferon induction. These improvements were apparent in cow but not
232 chicken cells, indicative of evolutionary adaptations to the new host. This is consistent with
233 other studies showing a replicative advantage of cattle isolates over an avian precursor [8,
234 29]. For PB2 and PA, the amino acid mutations PB2 M631L and PA K497R present in the
235 Cattle Texas strain we used have recently been reported to enhance polymerase efficiency
236 and virus replication in cow mammary cells [3, 17, 19]. Furthermore, impairment to
237 transcriptional efficiencies rendered by the newly acquired segment 5 imply that there is still
238 the potential for further fitness gains of the B3.13 genotype in cattle.

239 Pigs are the classic mixing vessel of IAV, the respiratory tract of which is unusual in its
240 ability to support infection with both avian and mammalian IAV strains and from which the

241 most recent influenza pandemic in 2009 arose [31, 32]. However, HPAI H5 infections in pigs
242 are rare; pigs were either not susceptible to H5N1 2.3.4.4b strains following nasal exposure
243 [33], or when infected no transmission was observed [34]. Therefore, reassortment of H5 HPAI
244 with other mammalian IAV strains within the swine respiratory tract can be considered unlikely.
245 However, our observations on the ability of avian and mammalian IAV strains to infect cow
246 mammary glands raised the question of whether cow udders could serve as mixing vessels
247 for the generation of novel strains containing human-adapted and H5 HPAI-origin segments,
248 analogous to the pig reassortment events that are conjectured to have precipitated previous
249 pandemics. The fact that cow mammary cells can be co-infected with human and avian IAV
250 strains supported by the mixed distribution of α-2,3 and α-2,6 linked sialic acid observed in
251 these cells, indicates that cow udders do have this potential.

252 Infection of cows with human and other IAV strains has been suggested in the past. In
253 1997, dairy cows in the southwest of England presented with sporadic drops in milk
254 production, which the reporting authors considered to be attributable to IAV [35, 36]. Additional
255 studies have reported seroconversion against circulating seasonal H3N2 virus in British cattle,
256 which was associated with reduced milk yield and respiratory disease [37, 38]. Despite the
257 occasional respiratory signs, such as nasal discharge and increased respiratory rate followed
258 by seroconversion, virus isolation from respiratory swabs from these seroconverted animals
259 was unsuccessful. With hindsight, isolation from milk may have had a higher chance of
260 success. Consequently, the idea that “cows could foster flu pandemics” was considered back
261 in the early 2000s [39]. Moreover, the recent seroconversion for H5N1 2.3.4.4b in sheep and
262 detections of IAV RNA in milk [40, 41] further suggests that other ruminant livestock species
263 may hold similar potential.

264 Overall, our findings point to requirements for reconfigured and enhanced policy
265 procedures and surveillance of IAV incursions into ruminant livestock species. Currently,
266 mastitis outbreaks are not routinely investigated for the presence of IAV. Adding IAV testing
267 to mastitis diagnostic assessments as a differential when other common causes have been
268 excluded will be beneficial to livestock. This will allow early detection of emerging events with

269 implementation of appropriate infection control measures and justify contact tracing of farm
270 workers.
271

272 Materials and Methods

273 Ethics

274 All reverse genetics work used a loss-of-function approach and was carried out under
275 a license (GMRA1811) from the UK Health & Safety Executive. All work with avian viruses
276 was carried out in a segregated BSL2 laboratory in the Roslin Institute, separate from where
277 mammalian IAV strains are handled.

278 All animal experimental work was completed under license and in accordance with the
279 Animal (Scientific Procedures) Act 1986 and with approval from the Roslin Institute animal
280 welfare and ethics committee under the project licence number PP0612543. All studies were
281 performed in line with the Animal Research: Reporting of *In Vivo* Experiments (ARRIVE)
282 Guidelines [42].
283

284 Cell line maintenance, primary cell isolation, derivation and culture

285 Madin-Darby Canine Kidney (MDCK) (American Type Culture Collection, ATCC),
286 MDCK expressing galline ANP32A (MDCK-GgANP32A) [43], MDCK expressing
287 Sialyltransferase 1 (MDCK-SIAT) [44], human embryonic kidney (HEK293T) and immortalised
288 mammary epithelial cells (MAC-T) [45] were cultured in DMEM supplemented with 10% foetal
289 bovine serum (FBS), 2mM glutamine, 100 U/ml penicillin, and 100 µg/ml streptomycin. MDCK-
290 SIAT cells were further supplemented with 50 µg/ml geneticin. MAC-T cells were further
291 supplemented with 5 µg/ml insulin and 1 µg/ml hydrocortisone. Chicken lung cells (CLEC213)
292 [46] were cultured with DMEM/Nutrient Mixture F-12 also supplemented with 8% FBS, 100
293 U/ml penicillin and 100µg/ml streptomycin. BAT-II cells [47, 48] were maintained in Small
294 Airway Growth medium (Lonza) further supplemented with 10% FBS, 100 U/ml penicillin and

295 100µg/ml streptomycin. All immortalised cells were regularly tested for mycoplasma
296 contamination and passaged once or twice weekly.

297 Primary cow mammary epithelial cell (bMEC) lines generated from the mammary
298 glands of Aberdeen Angus cross cows as previously described [49]. Glands were sprayed with
299 70% ethanol and skin was removed. Cuboidal epithelial tissue fragments (5 cm in length) were
300 cut from the gland, submerged in 70% ethanol for 30s and washed 5 times in PBS containing
301 antibiotics and 2.5 µg/ml amphotericin B. Tissue fragments were transferred to a glass petri
302 dish and minced with scalpels to 2-3 mm pieces. Next, 10-15g of minced tissue was
303 dissociated overnight with low shaking in 20 ml of DMEM/Nutrient Mixture F-12 supplemented
304 with 15 mM HEPES and 0.075% sodium bicarbonate, 2% Bovine serum albumin (BSA), 300
305 U/ml Collagenase Type I and 100 U/ml Hyaluronidase from bovine testes. Dissociation media
306 was removed by centrifugation and pellet was washed twice with DMEM/F12. This yielded
307 small aggregates of part-digested tissue which were resuspended in freezing medium and
308 stored at -150ºC. To obtain a single cell suspension, aliquots of part-digested tissue
309 aggregated were thawed, washed with Hanks' Balanced Salt Solution (HBSS) supplemented
310 with 2% FBS, resuspended in warm trypsin and vigorously pipetted for 3 mins and washed
311 with HBSS/2% FBS, resuspended in a warm Dispase/DNAse solution and gently pipetted for
312 3 minutes. Ice cold HBSS/ 2% FBS was added and the suspension was filtered on a 70 µM
313 strainer, cells were washed by centrifugation, resuspended in growth media (DMEM/F12
314 supplemented with 0.1% BSA, 10 ng/ml epidermal growth factor (EGF), 10 ng/ml cholera toxin,
315 1 µg/ml bovine insulin, 0.5 µg/ml hydrocortisone, 100 U/ml penicillin, 100 µg/ml streptomycin
316 and 250 µg/ml gentamycin) and seeded onto collagen coated wells/flasks. bMECs were
317 examined everyday by light microscopy to check for signs of contamination, viability,
318 morphology, and confluence. Media was refreshed daily. Growth media was further
319 supplemented with 2.5 µg/ml amphotericin B, the concentration of which was halved every
320 day until the cells had reached sufficient confluency to be expanded.

321 Primary fibroblasts were extracted from skin and brain tissue explants dissociated with
322 5 mg/ml Collagenase type I at 37ºC, shaking for 3h. The dissociated material was passed

323 through a 70 µm filter and washed with HBSS. Cells were cultured on bovine gelatine-coated
324 tissue culture plastic and expanded in Glasgow's MEM) supplemented with 10% foetal bovine
325 serum, 2 mM L-glutamine, 1x MEM non-essential amino acids, 1 mM sodium pyruvate, 0.1 mM
326 2-mercaptoethanol, 100 U/ml penicillin-streptomycin, 50 µg/ml gentamicin and 2.5 µg/ml
327 amphotericin B. Established cultures were maintained in the same medium without antibiotics.
328 Cow PBMCs were collected from Holstein-Friesian cattle housed at the University of
329 Edinburgh farm using published procedures [50]. Cow blood derived macrophages (BDΦ)
330 were generated from PBMCs as described previously [50] except that the macrophages were
331 cultured in BDΦ medium (RPMI-1640 supplemented with 20% FBS, 4 mM L-glutamine and
332 50 µM β-mercaptoethanol, 100 U/ml penicillin-streptomycin and 20 ng/ml His-tagged
333 recombinant bovine CSF1 - the latter supplied by the Roslin Immunological Toolbox). BDΦ
334 medium was replaced on day 7. On day 12 the adherent cells were rigorously washed with
335 phosphate-buffered saline PBS and detached with TrypLE Express. Purified BDΦs were
336 resuspended at 1.5 x 10^5 cells/ml in BD Φ medium without CSF1, aliquoted into 24 well plates
337 (1ml/well) and cultured for 48h before infection on day 14.
338 Bovine 3D enteroids were derived from five 6-month-old healthy male British Holstein–
339 Friesian calves housed at the University of Edinburgh farm. Calves were subject to Schedule
340 1 method of cull and sections of distal ileum were obtained post-mortem and stored in HBSS
341 on ice until further use. Crypts were isolated and 3D enteroids were cultured as previously
342 described [51]. Bovine 3D organoid cultures were used to generate 2D enteroids as previously
343 described [52].
344 Bovine mammary gland explants were extracted from udder tissue collected at
345 Sandyford Abattoir (Paisley, Scotland) from healthy lactating cows that had been culled for
346 the food chain. Excess tissue was removed, teat and gland cistern were dissected and
347 transferred to transport media comprising of chilled DMEM supplemented with 100 µg/ml
348 Penicillin/ 100 µg/ml streptomycin and 5 µg/ml fungizone. Every 45 minutes, tissues were
349 transferred to 500 ml of fresh transport media. Inside class II biological safety cabinet, explants

350 were made using a 5mm biopsy punch. Biopsies were added to 24 well plates with 500ul of
351 transport media further supplemented with 10% FBS and incubated for 24h at 37ºC, 5% CO_2
352 prior to infection.

353 Validation of bovine origin of the primary and continuous cell lines was performed by
354 PCR. DNA was extracted from cell pellets, and the cytochrome B gene was amplified by PCR
355 with degenerate primers (CGAGACGTVAAYTAYGGMTGA and
356 ACBGTDGCYCCTCARAADGATATTTG). Cycling conditions were 94°C for 2 minutes,
357 followed by 50 cycles of 94°C for 18 seconds, 50°C for 21 seconds then 72°C for 30 seconds
358 with a final extension of 72°C for 5 minutes. Amplicons were sent for Sanger sequencing and
359 resultant sequences were aligned to the Bos taurus mitochondrion complete genome
360 reference sequence (NCBI accession number NC_006853.1).

361 All cells, organoids and explants were kept at 37˚C and 5% CO_2 under normoxic
362 conditions.

363

364 **Viruses**

365 A/Puerto Rico/8/1934 H1N1 (“PR8”) [53], mouse adapted A/California/04/2009 H1N1
366 (“Cal04”) [54], A/WSN/33 H1N1 (“WSN”), swine adapted A/mallard/Netherlands/10-Cam/1999
367 H1N1 (“Mallard”) [55], A/Udorn/307/1972 H3N2 (“Udorn”), A/England/195/2009 pH1N1
368 (“Eng195”), A/swine/England/87842/1990 H3N2 (“Swine H3N2”) and 2:6 reassortants of
369 2.3.4.4b H5N1 viruses containing PR8 segments 4 and 6 viruses were generated by reverse
370 genetics as previously described [56]. Briefly, 2×10^6 HEK293T cells were transfected in
371 OptiMEM with pDUAL reverse genetics plasmids (250 ng of plasmid for each virus segment),
372 using 4 µl of Lipofectamine 2000 according to the manufacturer’s instructions. At 24 hours
373 post transfection, the media was replaced by serum-free DMEM supplemented with 0.14%
374 (w/v) fraction V BSA and 1 µg/ml of l-(tosylamido-2-phenyl) ethyl chloromethyl ketone (TPCK)-
375 treated trypsin. Virus-containing supernatant was collected after a further 2-days incubation
376 (here described as a “P0 stock”). P0 stocks of PR8, Swine H3N2 and Udorn were propagated
377 in MDCK cells. P0 stocks of Mallard, Eng195 and PR8 2:6 2.3.4.4b H5N1 reassortants were

378 further propagated in 10-day embryonated hen's eggs. Allantoic fluids were collected 48hpi.
379 Cal04 P0 stocks were propagated in MDCK-SIAT cells. Reassortants between A/dairy
380 cattle/Texas/24-008749-001-original/2024 H5N1 ("Cattle Texas") and
381 A/chicken/England/053052/2021 H5N1 ("AIV07") were propagated in MDCK-GgANP32A.
382 Isolates of A/USSR/90/1977 H1N1 ("USSR") A/Brisbane/10/2007 H3N2 ("Brisbane"),
383 A/Norway/3433/ 2018 H1N1 ("Norway") and A/swine/453/England/2006 H1N1 ("Swine H1N1")
384 isolates were propagated in MDCK cells. Clarified supernatants were typically collected at 36–
385 72 hpi. Isolates of A/chicken/Belgium/460/2019 H3N1 ("H3N1"), A/chicken Belgium/150/1999
386 H5N2 ("H5N2"), A/chicken/Netherlands/917/2010 H6N1 ("H6N1") and A/chicken/Saudi
387 Arabia/2525/2000 H9N2 ("H9N2") isolates were propagated in hen's eggs and allantoic fluids
388 were collected and clarified at 48 hpi. All viruses were sequenced to confirm identity using
389 Nanopore sequencing (described below).
390
391 **Table 1: Virus strains, abbreviations and uses in this study.**

Virus strain name	Abbreviation	Panel	GISAID ID	Type of virus/assay
A/Puerto Rico/8/1934 H1N1	PR8	Lab-adapted		Whole virus, minireplicon
A/WSN/33 H1N1	WSN	Lab-adapted		Whole virus
A/California/04/2009 H1N1	Cal04	Lab-adapted		Whole virus, minireplicon
A/mallard/Netherlands/10-Cam/1999 H1N1	Mallard	Lab-adapted		Whole virus, minireplicon
A/USSR/90/1977 H1N1	USSR	Human		Whole virus
A/Udorn/307/1972 H3N2	Udorn	Human		Whole virus, minireplicon
A/Brisbane/10/2007 H3N2	Brisbane	Human		Whole virus
A/England/195/2009	Eng195	Human	EPI_ISL_29994	Whole virus, minireplicon

A/Norway/3433/2018 H1N1	Norway	Human	EPI_ISL_391292	Whole virus
A/swine/453/England/2006 H1N1	Swine H1N1	Swine		Whole virus
A/swine/England/87842/1990 H3N2	Swine H3N2	Swine		Whole virus
A/chicken/Belgium/460/2019 H3N1	H3N1	Avian		Whole virus, minireplicon
A/chicken Belgium/150/1999 H5N2	H5N2	Avian		Whole virus
A/chicken/Netherlands/917/2010 H6N1	H6N1	Avian		Whole virus
A/chicken/Saudi Arabia/2525/2000 H9N2	H9N2	Avian		Whole virus
A/duck/Tripura/103597/2008 H5N1	Tripura	Avian		Minireplicon
A/chicken/England/030786/2020	H5N8-20	2.3.4.4b H5N1		PR8 2:6 reassortant
A/chicken/England/053052/2021 H5N1	AIV07	2.3.4.4b H5N1	EPI_ISL_9012457	PR8 2:6 reassortant, minireplicon
A/chicken/Scotland/054477/2021 H5N1	AIV09	2.3.4.4b H5N1	EPI_ISL_9012696	PR8 2:6 reassortant
A/chicken/England/085598/2022 H5N1	AIV48	2.3.4.4b H5N1	EPI_ISL_13782459	PR8 2:6 reassortant, minireplicon
A/dairy cattle/Texas/24-008749-001-original/2024 H5N1	Cattle Texas	2.3.4.4b H5N1	EPI_ISL_19094762	PR8 2:6 reassortant, minireplicon

392

393 **RNA extraction and Multi-segment RT-PCR**

394 To confirm the genome sequences of the virus strains used, viral RNA was extracted
395 from cell- and egg-grown viral stocks using the QIAamp Viral extraction mini kit (QIAGEN) as
396 per manufacturer's instructions. Viral genomes were amplified using the Superscript III One-
397 Step RT-PCR kit (Invitrogen), 5 µl of extracted viral RNA, GGGGGGAGCAAAAGCAGG and
398 GGGGGGAGCGAAAGCAGG as forward and GGGGTTATTAGTAGAAACAAGG as reverse
399 primers [57]. Thermocycling conditions for RT-PCR reaction were: 55°C for 2 mins, 42°C for

400 60 mins, 94°C for 2 mins; 5 cycles of 94°C for 30 s, 44°C for 30 s and 68°C for 3 mins 30 s;
401 26 cycles of 94°C for 30 s, 57°C for 30 s and 68°C for 3 mins 30 s and 10 mins hold at 68°C.
402 Resulting PCR was analysed on an 1% agarose gel
403
404 **Nanopore sequencing and data analysis**
405 RT-PCR products were pooled and prepared for sequencing using a ligation
406 sequencing amplicon kit (SQK-NBD114.24, Oxford Nanopore Technologies, Oxford, UK) and
407 sequenced on a FLO-MIN114 flow cell (R10.4.1., Oxford Nanopore Technologies) on an in-
408 house GridION device. Final library concentration was approximately 10 fmol. Molarity was
409 determined using Oxford Nanopore recommended tables, assuming an average multi-
410 segment RT-PCR fragment size of 1.3 kb. Reads were called using the high accuracy basecall
411 setting on the MinKNOW UI (Oxford Nanopore Technologies). The "passed" FASTQ output
412 files were used in the sequencing analysis. Data was analysed using the EPI2ME (Oxford
413 Nanopore Technologies) and Sequeduct (Edinburgh Genome Foundry) [58]pipelines. The
414 processed FASTQ files were aligned against expected sequences. For the Sequeduct
415 pipeline, reference sequences were converted to Genbank format. Consensus sequence
416 output from the "analysis" workflow was used to align against expected sequences.
417
418 **Plaque assays**
419 Confluent monolayers of MDCK cells (1×10^6 cells seeded in 12-well plates the day
420 prior to infection) were washed once with PBS, then infected with 250 µl of tenfold serial
421 dilutions of virus. Following a 1 h incubation at 37 °C that allowed virus adsorption, cells were
422 overlaid with DMEM supplemented with 0.14% fraction V BSA, 1 µg/ml TPCK-treated trypsin
423 and 1.2% Avicel. Following a 48h undisturbed incubation at 37 °C, cells were fixed with 10%
424 Neutral Buffered Formalin for at least 20 minutes and stained with a 0.1% toluidine blue
425 solution for at least 1 h and plaques were then counted. Plaque assays for avian viruses or
426 PR8 2:6 viruses with avian origin PB2 were performed as described but using MDCK-

427 GgANP32A cells. Plaque assays for human viruses Eng195, Cal04, Brisbane and Norway
428 H1N1 were performed using MDCK-SIAT cells and incubation temperatures of 35 °C for 72h.
429

430 **Virus replication kinetics**

431 Monolayers of cells were washed once with PBS and infected with virus diluted in
432 serum-free medium for 1 h at 37 °C (the multiplicity of infections used is specified in each figure
433 legend). Infectious medium was replaced with serum-free medium supplemented with 0.14%
434 fraction V BSA and 1 µg/ml TPCK-treated bovine pancreas trypsin.

435 Individual mammary explants were transferred to 96-well plates and infected with 5000
436 PFU of virus in 100 µl of serum free DMEM for 2h at 37ºC. Explants were transferred to clean
437 24-well plates, washed 3x with warm PBS and overlayed with 1ml of DMEM supplemented
438 with 0.14% fraction V BSA and 1µg/ml TPCK. Supernatant was collected at different
439 timepoints post infection and infectious titres were determined by plaque assay.
440

441 **Immunoblotting**

442 Cells were lysed in Laemmli buffer, heated at 80 °C for 5 min and subjected to
443 polyacrylamide gel electrophoresis using sodium dodecyl sulfate-based buffer. Peptides were
444 transferred to polyvinylidene difluoride membranes for 90 minutes at 32 V. Membranes were
445 blocked for 1 h with 1× Tris-buffered saline with 0.1% Tween20 (TBST)/5% milk, washed three
446 times with TBST and stained with primary antibodies diluted in TBST/5% BSA overnight at
447 4 °C. After three 5-minute TBST washes, secondary antibodies were diluted in blocking buffer
448 and incubated for 1 h at room temperature protected from direct light. Following three more
449 washes in TBST, membranes were imaged using the LI-COR Fc-Odyssey Imaging platform
450 using the Image Studio Lite Software.
451

452 **Plasmid-based IFN- β promoter reporter assays**

453 Under confluent monolayers of MAC-T or CLEC213 cells were co-transfected with
454 500ng or 100 ng of reporter plasmid encoding firefly luciferase under the control of human [59]

455 or chicken IFN-β [60] promoter and 1000ng of segment 8 pDUAL plasmids using 2 µl of
456 Lipofectamine 2000. 24 hours post transfection, cells were stimulated with 5 µg of Poly I:C by
457 transfection using 2 µl of Lipofectamine/well. Mock-stimulated cells were also included where
458 Poly I:C was replaced by water. 24 hours post-stimulation, cells were lysed with 100 µl of
459 reporter lysis buffer and luciferase activity was measured from 40 µl of lysate in opaque 96-
460 well plates by using 25 µl of luciferase assay reagent in Cytation3 Plate Reader and Imager
461 (integration time 1 second).
462
463 **Cellular gene expression shutoff transfection-based assays**
464 Sub-confluent monolayers of MAC-T and CLEC213 cells were co-transfected in
465 triplicate with a range of pDUAL segment 3 or 8 effector plasmids and 200ng of pRL using
466 2µL of Lipofectamine2000. Forty eight hours post transfection, cells were lysed and renilla
467 luciferase expression was quantified using a Renilla Luciferase Assay kit. Briefly, cells were
468 lysed with 100µL of 1× lysis buffer and frozen overnight at -20°C. Cells were scraped off the
469 plate, cell debris was removed by centrifugation (8000rpm, 5 minutes, 4°C). Luminescence
470 was measured from the mix of 20 µl of lysate and 50 µl of 1× Renilla luciferase substrate using
471 a Cytation3 Plate Reader and Imager (integration time 1 second).
472
473 **Puromycin-labelling of nascent proteins**
474 Subconfluent monolayers of MAC-T cells were infected at MOI 5. At 9, 12, 15 and 18
475 hpi, supernatant was replaced with fresh medium supplemented with 20 µg/ml of puromycin
476 dihydrochloride for 1h. Cells were washed twice with PBS, lysed in Laemmli buffer and
477 subjected to immunoblotting using a primary anti-puromycin antibody (Millipore; MABE343).
478
479 **RNP reconstitution (minireplicon) assays**
480 Sub-confluent monolayers of MAC-T or CLEC213 cells (1×10^5 cells seeded in 24-well
481 plates the previous day) were co-transfected in triplicate with 50 ng of each pDUAL plasmid
482 encoding PB2, PB1, PA and NP along with 20 ng of a bovine PolI-driven vRNA-like firefly

483 luciferase reporter plasmid [17]. As negative controls, transfections lacking the PB2 plasmid
484 (with empty pDUAL vector used to balance plasmid amount) were also performed. Two days
485 post transfection, cells were lysed with 120 µl of reporter lysis buffer (Promega E4030).
486 Lysates were cleared and luminescence was measured from 40 µl of lysate in opaque 96-well
487 plates by using 25 µl of luciferase assay reagent in a Cytation3 Plate Reader and Imager
488 (integration time 1 second).
489
490 **Tissue homogenisation**
491 Mammary explants were added to 1ml of serum-free DMEM and a 5mm diameter
492 stainless steel bead in 2ml tubes and homogenised using a Tissue Lyser II (Qiagen) system
493 at 28kHz for 3 sets of 2 minutes. Homogenised tissue was clarified by centrifugation (3000
494 rpm, 5 min, 4°C). Homogenates were titrated for infectious virus by plaque assay.
495
496 **Glycomic analysis of MAC-T and bMEC cells**
497 Approximately 10 million cultured MAC-T and bMEC cells were washed and scraped
498 into cold PBS. Cells were then pelleted and washed several times with cold PBS prior to
499 processing [61]. Briefly, cells were lysed by sonication, dialysed and lyophilised. Reduction
500 and carboxymethylation reactions were carried out on the lyophilised material, which was
501 subsequently dialysed and lyophilised. Samples were digested with trypsin (Sigma) and the
502 resultant glycopeptides purified by Sep-Pak C18 chromatography. N-glycans were released
503 by PNGase-F (Roche) and purified by Sep-Pak C18 chromatography. N-glycan samples were
504 then split into three aliquots. Two of the three aliquots were treated with either sialidase-S or
505 sialidase-A (Agilent Technologies) and then purified by C18 Sep-Pak chromatography, the
506 third aliquot was untreated. Untreated and treated glycans were then permethylated and
507 analysed using a 4800 MALDI-TOF mass spectrometer (Applied Biosystems).
508 MS and MS/MS data were visualised using Data Explorer (Applied Biosystems) and
509 $[M + Na]^+$ molecular ions were annotated manually with the assistance of GlycoWorkbench
510 [62]. Glycan structures were predicted based on composition and knowledge of biosynthetic

511 pathways, with MS/MS analysis used to confirm assignments. Figures were prepared using
512 Adobe Illustrator.

513 Glycomic data was quantified using an R programme described in Wu et al., 2024 [63]
514 which detects glycans according to their isotopic peak pattern and calculates the relative
515 intensity across the isotope cluster. An R programme was then used to calculate the
516 proportions of α-2,3 and α–2,6 sialic acid. First, the relative intensity of each glycan was
517 normalised to the sum of the relative intensities of all the glycans in the sample. For sialylated
518 glycans, normalised intensities were then weighted based on the number of sialic acid
519 residues present on each glycan. The proportion of α-2,6 linked sialic acid was determined by
520 summing the weighted normalised intensities of sialylated molecular ion peaks remaining after
521 sialidase-S digestion. The proportion of α-2,3 linked sialic acid was calculated by subtracting
522 the weighted normalised intensities of sialylated molecular ions in the sialidase-S sample from
523 the weighted normalised intensities of sialylated molecular ions from the untreated sample
524 (raw data in Supplementary File) [64].

525

526 **Cell staining and flow cytometry**

527 Infected bMECs were trypsinised, resuspended and fixed in PBS/4% formaldehyde.
528 Following a PBS wash by centrifugation, cells were blocked with PBS/2%BSA for 1h. Cells
529 were stained with rabbit anti-H3 (c33) or mouse anti-H1 (2-12C, absolute antibody) primary
530 antibodies diluted 1:5000 in blocking buffer for 1h at room temperature and with constant
531 agitation. Cells were then washed twice 2x with blocking buffer and resuspended in a
532 secondary antibody solution containing donkey anti-rabbit647 (ab150075, abcam) and donkey
533 anti-mouse 488 (A11011, Invitrogen) for another 30 min. Cells were centrifuged, washed twice
534 with blocking buffer and analysed using a BD LSR Fortessa X20 cytometer.

535

536

537

538 **Acknowledgments**

539 The authors would like to thank Prof Massimo Palmarini (MRC-University of Glasgow
540 Centre for Virus Research) and Dr John McCauley (recently retired from Crick Institute) for
541 providing MDCK-GgANP32A and MDCK-SIAT cells, respectively. BAT-II cells were kindly
542 provided by Dr Diane Lee (University of Surrey). Chicken lung cells (CLEC213) were kindly
543 provided by Dr Sascha Trapp of the INRA Centre Val de Loire. We thank Dr Laurence Tiley
544 (The University of Cambridge), Dr Ron Fouchier (Erasmus MC) and Dr Daniel Perez (The
545 University of Georgia) for providing the reverse genetics systems for
546 A/mallard/Netherlands/10-Cam/1999 (H1N1), A/Puerto Rico/8/1934 (H1N1) and
547 A/California/04-061-MA/2009 (H1N1) viruses, respectively, as well as colleagues at the
548 Animal and Plant Health Agency for early provision of viral genetic data to the FluMap
549 consortium. Human IFN-β::firefly luciferase and chicken IFN2::firefly luciferase reporter
550 plasmids were kindly gifted by Prof Richard Randall (University of St Andrews) and Dr Holly
551 Shelton (previously at Pirbright Institute), respectively. We gratefully acknowledge the expert
552 assistance of staff at the University of Edinburgh Large Animal Research Imaging Facility and
553 Langhill Farm.

554

555 **Funding**

556 UK Biotechnology and Biological Sciences Research Council grant BB/CCG2270/1 (The
557 Roslin Immunological Toolbox)

558 UK Biotechnology and Biological Sciences Research Council Institute Strategic Programme
559 funding grants BBS/E/RL/230002A and BBS/E/RL/230002C (RMP, JRF, JH, JS, TB, KS, FXD,
560 EG and PD)

561 UK Biotechnology and Biological Sciences Research Council Institute Strategic Programme
562 funding grant BBS/E/PI/230002B and National Bioscience Research Infrastructure funding
563 BBS/E/PI/23NB0004 and BBS/E/PI/23NB0003 (TPP, IB and MI)

564 UK Biotechnology and Biological Sciences Research Council grant BB/V004697/1 (PRM)

UK Biotechnology and Biological Sciences Research Council grant BB/V011286/1 (PD)

UK Natural Environment Research Council (NERC) Capability to Deliver funding NE/Y001591/1 (EG and PD)

UK Medical Research Council FluTrailMAP-One Health consortium grant MR/Y03368X/1 (RMP, TPP, IB, WB, DHG, MI, PRM, SMH and PD

UK Biotechnology and Biological Sciences Research Council and UK Department for Environment, Food & Rural Affairs FluMap consortium grants BB/X006123/1 and BB/X006166/1 (PD, MI)

UK Biotechnology and Biological Sciences Research Council and UK Department for Environment, Food & Rural Affairs FluTrailmap consortium grants BB/Y007352/1 and BB/Y007298/1 (RMP, EG, PD, TPP, IB, MI)

UK Biotechnology and Biological Sciences Research Council and Department of Biotechnology, Government of India grants BB/L004666/1 and BT/IN/Indo-UK/FADH/48/AM/2013 (AAR, AM and PD).

UK Biotechnology and Biological Sciences Research Council and Department of Biotechnology and ERA-net ICRAD project FluNuance grant number BB/V0119899/1 (SdW, KS and PD)

Wellcome Trust Sir Henry Dale fellowship award 211222/Z/18/Z (EG).

UK Academy of Medical Sciences Springboard Grant 1049 (DHG)

University of Edinburgh Chancellor's Fellowship (RMP)

Roslin Foundation PhD studentship (MB)

UK Biotechnology and Biological Sciences Research Council EastBio Doctoral Training Partnership PhD studentship BB/T00875X/1 (AM).

Credit contributions

Rute Maria Pinto – RMP – Conceptualisation, Methodology, Validation, Formal analysis, Investigation, Resources, Data curation, Visualisation, Writing – original draft, Writing – reviewing and editing, Supervision, Project administration, Funding acquisition

Colin P Sharp – CS -Conceptualisation, Methodology, Validation, Investigation, Resources, Data curation, Writing – reviewing and editing, Supervision, Project administration

Maia Beeson – MB – Methodology, Validation, Investigation, Data curation, Writing – reviewing and editing

Nunticha Pankaew – NP – Methodology, Validation, Investigation, Data curation, Writing – reviewing and editing

Jack A. Hassard - JAH – Methodology, Validation, Formal analysis, Investigation, Data curation, Visualisation, Writing – original draft, Writing – reviewing and editing

Alexander Moxom – AM – Methodology, Validation, Investigation, Writing – original draft, Writing – reviewing and editing

Callum Magill – CM – Methodology, Validation, Investigation, Writing – original draft

Laura Tuck – LT – Methodology, Validation, Writing – reviewing and editing

Stephen Meek – SM – Methodology, Writing – reviewing and editing

Hui Min Lee – HML – Methodology, Resources

Kirsty Jensen – JK – Methodology, Writing – reviewing and editing

Inga Dry – ID – Methodology, Validation, Writing – reviewing and editing

Pedro Melo – PM – Methodology, Resources, Writing – reviewing and editing

Jiayun Yang – JY .- Methodology, Resources, Writing – reviewing and editing

Ashwin Ashok Raut – AAR - Resources

Anamika Mishra – AM - Resources

Sjaak de Wit – SdW – Resources, Writing – reviewing and editing

J. Ross Fitzgerald – JRF – Methodology, Resources, Writing – reviewing and editing, Funding acquisition

Jayne C. Hope – JCH – Methodology, Resources, Writing – reviewing and editing, Funding acquisition

Joanne Stevens – JS – Methodology, Resources, Funding acquisition

Tom Burdon – TB – Methodology, Resources, Funding acquisition

Kate Sutton – KS – Methodology, Resources, Writing – reviewing and editing, Funding acquisition

Cristina L. Esteves – CLE – Methodology, Resources

F. Xavier Donadeu – FXD – Methodology, Resources, Writing – reviewing and editing, Funding acquisition

Thomas P. Peacock – TPP – Methodology, Writing – reviewing and editing, Funding acquisition.

Ian Brown - IB - Project administration, Funding acquisition

Wendy Barclay – WB - Project administration, Funding acquisition

Daniel H. Goldhill – DHG – Methodology, Resources, Writing – reviewing and editing, Funding acquisition

Munir Iqbal – MI – Methodology, Resources, Writing – reviewing and editing, Funding acquisition

Pablo R. Murcia – PMR – Methodology, Resources, Writing – reviewing and editing, Funding acquisition

Stuart M. Haslam – SMH – Methodology, Resources, Supervision, Project administration, Funding acquisition

Eleanor Gaunt – EG – Conceptualisation, Methodology, Resources, Data curation, Visualisation, Writing – original draft, Writing – reviewing and editing, Supervision, Project administration, Funding acquisition

Paul Digard – PD – Conceptualisation, Methodology, Resources, Data curation, Writing – original draft, Writing – reviewing and editing, Supervision, Project administration, Funding acquisition

References

1. Bellido-Martín, B., et al., *Evolution, spread and impact of highly pathogenic H5 avian influenza A viruses.* Nature Reviews Microbiology, 2025.
2. Baker, A.L., et al., *Dairy cows inoculated with highly pathogenic avian influenza virus H5N1.* Nature, 2025. **637**(8047): p. 913-920.
3. Nguyen, T.-Q., et al., *Emergence and interstate spread of highly pathogenic avian influenza A(H5N1) in dairy cattle in the United States.* Science, 2025. **388**(6745): p. eadq0900.
4. Caserta, L.C., et al., *Spillover of highly pathogenic avian influenza H5N1 virus to dairy cattle.* Nature, 2024. **634**(8034): p. 669-676.
5. Sreenivasan, C.C., et al., *Influenza A in Bovine Species: A Narrative Literature Review.* Viruses, 2019. **11**(6): p. 561.
6. Burrough, E.R., et al., *Highly Pathogenic Avian Influenza A(H5N1) Clade 2.3.4.4b Virus Infection in Domestic Dairy Cattle and Cats, United States, 2024.* Emerg Infect Dis, 2024. **30**(7): p. 1335-1343.
7. Sanchez-Rojas, I.C., et al., *Highly Pathogenic Avian Influenza (H5N1) Clade 2.3.4.4b in Cattle: A Rising One Health Concern.* Animals (Basel), 2025. **15**(13).
8. Octaviani, C.P., et al., *Superior replication, pathogenicity, and immune evasion of a Texas dairy cattle H5N1 virus compared to a historical avian isolate.* Scientific Reports, 2025. **15**(1): p. 8797.
9. Fabrizio, T.P., et al., *Genotype B3.13 influenza A(H5N1) viruses isolated from dairy cattle demonstrate high virulence in laboratory models, but retain avian virus-like properties.* Nature Communications, 2025. **16**(1): p. 6771.
10. Uyeki, T.M., et al., *Highly Pathogenic Avian Influenza A(H5N1) Virus Infection in a Dairy Farm Worker.* New England Journal of Medicine, 2024. **390**(21): p. 2028-2029.
11. Morse, J., et al., *Influenza A(H5N1) Virus Infection in Two Dairy Farm Workers in Michigan.* New England Journal of Medicine, 2024. **391**(10): p. 963-964.
12. Gu, C., et al., *A human isolate of bovine H5N1 is transmissible and lethal in animal models.* Nature, 2024. **636**(8043): p. 711-718.
13. Campbell, A.J., K. Brizuela, and S.S. Lakdawala, *mGem: Transmission and exposure risks of dairy cow H5N1 influenza virus.* mBio, 2025. **16**(3): p. e02944-24.
14. Jagger, B.W., et al., *An overlapping protein-coding region in influenza A virus segment 3 modulates the host response.* Science, 2012. **337**(6091): p. 199-204.
15. Mostafa, A., A. Nogales, and L. Martinez-Sobrido, *Highly pathogenic avian influenza H5N1 in the United States: recent incursions and spillover to cattle.* npj Viruses, 2025. **3**(1): p. 54.
16. Peacock, T.P., et al., *The global H5N1 influenza panzootic in mammals.* Nature, 2025. **637**(8045): p. 304-313.
17. Dholakia, V., et al., *Polymerase mutations underlie early adaptation of H5N1 influenza virus to dairy cattle and other mammals.* bioRxiv, 2025: p. 2025.01.06.631435.
18. Hale, B.G., et al., *The multifunctional NS1 protein of influenza A viruses.* Journal of General Virology, 2008. **89**(10): p. 2359-2376.
19. Mostafa, A., et al., *Avian influenza A (H5N1) virus in dairy cattle: origin, evolution, and cross-species transmission.* mBio, 2024. **15**(12): p. e02542-24.
20. Belshe, R.B., *The Origins of Pandemic Influenza — Lessons from the 1918 Virus.* New England Journal of Medicine, 2005. **353**(21): p. 2209-2211.

691 21. Harrington, W.N., C.M. Kackos, and R.J. Webby, *The evolution and future of influenza*
692 *pandemic preparedness.* Experimental & Molecular Medicine, 2021. **53**(5): p. 737-749.
693 22. Ríos Carrasco, M., et al., *The mammary glands of cows abundantly display receptors for*
694 *circulating avian H5 viruses.* Journal of Virology, 2024. **98**(11): p. e01052-24.
695 23. Nelli, R.K., et al., *Sialic Acid Receptor Specificity in Mammary Gland of Dairy Cattle Infected*
696 *with Highly Pathogenic Avian Influenza A(H5N1) Virus.* Emerg Infect Dis, 2024. **30**(7): p. 1361-
697 1373.
698 24. Nelli, R.K., et al., *Exploring influenza A virus receptor distribution in the lactating mammary*
699 *gland of domesticated livestock and in human breast tissue.* bioRxiv, 2025: p.
700 2025.04.16.649193.
701 25. Halwe, N.J., et al., *H5N1 clade 2.3.4.4b dynamics in experimentally infected calves and cows.*
702 Nature, 2025. **637**(8047): p. 903-912.
703 26. Palme , D.I., et al., *Strain-dependent variations in replication of European clade 2.3.4.4b*
704 *influenza A(H5N1) viruses in bovine cells and thermal inactivation in semi-skimmed or whole*
705 *milk.* Eurosurveillance, 2024. **29**(30): p. 2400436.
706 27. Xiong, J., et al., *Clade 2.3.4.4b highly pathogenic H5N1 influenza viruses from birds in China*
707 *replicate effectively in bovine cells and pose potential public health risk.* Emerging Microbes &
708 Infections, 2025. **14**(1): p. 2505649.
709 28. Bordes, L., et al., *H5N1 clade 2.3.4.4b avian influenza viruses replicate in differentiated bovine*
710 *airway epithelial cells cultured at air-liquid interface.* Journal of General Virology, 2024. **105**(6).
711 29. Imai, M., et al., *Highly pathogenic avian H5N1 influenza A virus replication in ex vivo cultures*
712 *of bovine mammary gland and teat tissues.* Emerging Microbes & Infections, 2025. **14**(1): p.
713 2450029.
714 30. Lowen Anice, C., et al., *Pandemic risk stemming from the bovine H5N1 outbreak: an account*
715 *of the knowns and unknowns.* Journal of Virology, 2025. **99**(4): p. e00052-25.
716 31. Schnitzler, S.U. and P. Schnitzler, *An update on swine-origin influenza virus A/H1N1: a review.*
717 Virus Genes, 2009. **39**(3): p. 279-292.
718 32. Ma, W., R.E. Kahn, and J.A. Richt, *The pig as a mixing vessel for influenza viruses: Human and*
719 *veterinary implications.* J Mol Genet Med, 2008. **3**(1): p. 158-66.
720 33. Graaf, A., et al., *Low Susceptibility of Pigs against Experimental Infection with HPAI Virus H5N1*
721 *Clade 2.3.4.4b.* Emerging Infectious Disease journal, 2023. **29**(7): p. 1492.
722 34. Kwon, T., et al., *Pigs are highly susceptible to but do not transmit mink-derived highly*
723 *pathogenic avian influenza virus H5N1 clade 2.3.4.4b.* Emerging Microbes & Infections, 2024.
724 **13**(1): p. 2353292.
725 35. Gunning, R.F. and G.C. Pritchard, *Unexplained sporadic milk drop in dairy cows.* Vet Rec, 1997.
726 **140**(18): p. 488.
727 36. Gunning, R., *Sporadic milk drop in dairy cows: a new causal agent to consider?* In Practice,
728 2002. **24**(8): p. 469-470.
729 37. Brown, I., et al., *Detection of antibodies to influenza virus A in cattle in association with*
730 *respiratory disease and reduced milk yield.* Veterinary Record, 1998. **143**(23): p. 637–638.
731 38. Crawshaw, T.R. and I. Brown, *Bovine influenza.* Vet Rec, 1998. **143**(13): p. 372.
732 39. Pearson, H., *Cows could foster flu pandemics.* Nature, 2002.
733 40. Government, U. *Influenza of avian origin confirmed in a sheep in Yorkshire*. 2025; Available
734 from: https://www.gov.uk/government/news/influenza-of-avian-origin-confirmed-in-a-
735 sheep-in-yorkshire.
736 41. Banyard, A.C., et al., *Detection of clade 2.3.4.4b H5N1 high pathogenicity avian influenza virus*
737 *in a sheep in Great Britain, 2025.* bioRxiv, 2025: p. 2025.06.27.661969.
738 42. Percie du Sert, N., et al., *The ARRIVE guidelines 2.0: Updated guidelines for reporting animal*
739 *research.* PLOS Biology, 2020. **18**(7): p. e3000410.
740 43. Pinto, R.M., et al., *BTN3A3 evasion promotes the zoonotic potential of influenza A viruses.*
741 Nature, 2023. **619**(7969): p. 338-347.

742 44. Matrosovich, M., et al., *Overexpression of the α-2,6-Sialyltransferase in MDCK Cells Increases*
743 *Influenza Virus Sensitivity to Neuraminidase Inhibitors.* Journal of Virology, 2003. **77**(15): p.
744 8418-8425.
745 45. Huynh, H.T., G. Robitaille, and J.D. Turner, *Establishment of bovine mammary epithelial cells*
746 *(MAC-T): an in vitro model for bovine lactation.* Exp Cell Res, 1991. **197**(2): p. 191-9.
747 46. Esnault, E., et al., *A novel chicken lung epithelial cell line: Characterization and response to low*
748 *pathogenicity avian influenza virus.* Virus Research, 2011. **159**(1): p. 32-42.
749 47. Lee, D. and M. Chambers, *A co-culture model of the bovine alveolus [version 2; peer review: 3*
750 *approved].* F1000Research, 2019. **8**(357).
751 48. Lee, D.F., et al., *Isolation and characterisation of alveolar type II pneumocytes from adult*
752 *bovine lung.* Scientific Reports, 2018. **8**(1): p. 11927.
753 49. Martignani, E., et al., *Bovine Mammary Organoids: A Model to Study Epithelial Mammary*
754 *Cells*, in *Epithelial Cell Culture: Methods and Protocols*, M. Baratta, Editor. 2018, Springer New
755 York: New York, NY. p. 137-144.
756 50. Mathie, H.A., et al., *Quantifying Mycobacterium avium subspecies paratuberculosis infection*
757 *of bovine monocyte derived macrophages by confocal microscopy.* Journal of Microbiological
758 Methods, 2020. **168**: p. 105779.
759 51. Hamilton, C.A., et al., *Development of in vitro enteroids derived from bovine small intestinal*
760 *crypts.* Veterinary Research, 2018. **49**(1): p. 54.
761 52. Sutton, K.M., et al., *Establishment of bovine 3D enteroid-derived 2D monolayers.* Vet Res,
762 2022. **53**(1): p. 15.
763 53. de Wit, E., et al., *Efficient generation and growth of influenza virus A/PR/8/34 from eight cDNA*
764 *fragments.* Virus Res, 2004. **103**(1-2): p. 155-61.
765 54. Ye, J., et al., *Variations in the Hemagglutinin of the 2009 H1N1 Pandemic Virus: Potential for*
766 *Strains with Altered Virulence Phenotype?* PLOS Pathogens, 2010. **6**(10): p. e1001145.
767 55. Bourret, V., et al., *Whole-genome, deep pyrosequencing analysis of a duck influenza A virus*
768 *evolution in swine cells.* Infection, Genetics and Evolution, 2013. **18**: p. 31-41.
769 56. Wise Helen, M., et al., *A Complicated Message: Identification of a Novel PB1-Related Protein*
770 *Translated from Influenza A Virus Segment 2 mRNA.* Journal of Virology, 2009. **83**(16): p. 8021-
771 8031.
772 57. Ip, H.S., et al., *An Evaluation of Avian Influenza Virus Whole-Genome Sequencing Approaches*
773 *Using Nanopore Technology.* Microorganisms, 2023. **11**(2): p. 529.
774 58. Vegh, P., et al., *Biofoundry-Scale DNA Assembly Validation Using Cost-Effective High-*
775 *Throughput Long-Read Sequencing.* ACS Synthetic Biology, 2024. **13**(2): p. 683-686.
776 59. King, P. and S. Goodbourn, *The beta-interferon promoter responds to priming through multiple*
777 *independent regulatory elements.* J Biol Chem, 1994. **269**(48): p. 30609-15.
778 60. James, J., et al., *The cellular localization of avian influenza virus PB1-F2 protein alters the*
779 *magnitude of IFN2 promoter and NFκB-dependent promoter antagonism in chicken cells.*
780 Journal of General Virology, 2019. **100**(3): p. 414-430.
781 61. Jang-Lee, J., et al., *Glycomic Profiling of Cells and Tissues by Mass Spectrometry: Fingerprinting*
782 *and Sequencing Methodologies*, in *Methods in Enzymology*. 2006, Academic Press. p. 59-86.
783 62. Ceroni, A., et al., *GlycoWorkbench: A Tool for the Computer-Assisted Annotation of Mass*
784 *Spectra of Glycans.* Journal of Proteome Research, 2008. **7**(4): p. 1650-1659.
785 63. Wu, G., et al., *Glycomics of cervicovaginal fluid from women at risk of preterm birth reveals*
786 *immuno-regulatory epitopes that are hallmarks of cancer and viral glycosylation.* Scientific
787 Reports, 2024. **14**(1): p. 20813.
788 64. Neelamegham, S., et al., *Updates to the Symbol Nomenclature for Glycans guidelines.*
789 Glycobiology, 2019. **29**(9): p. 620-624.

790

791

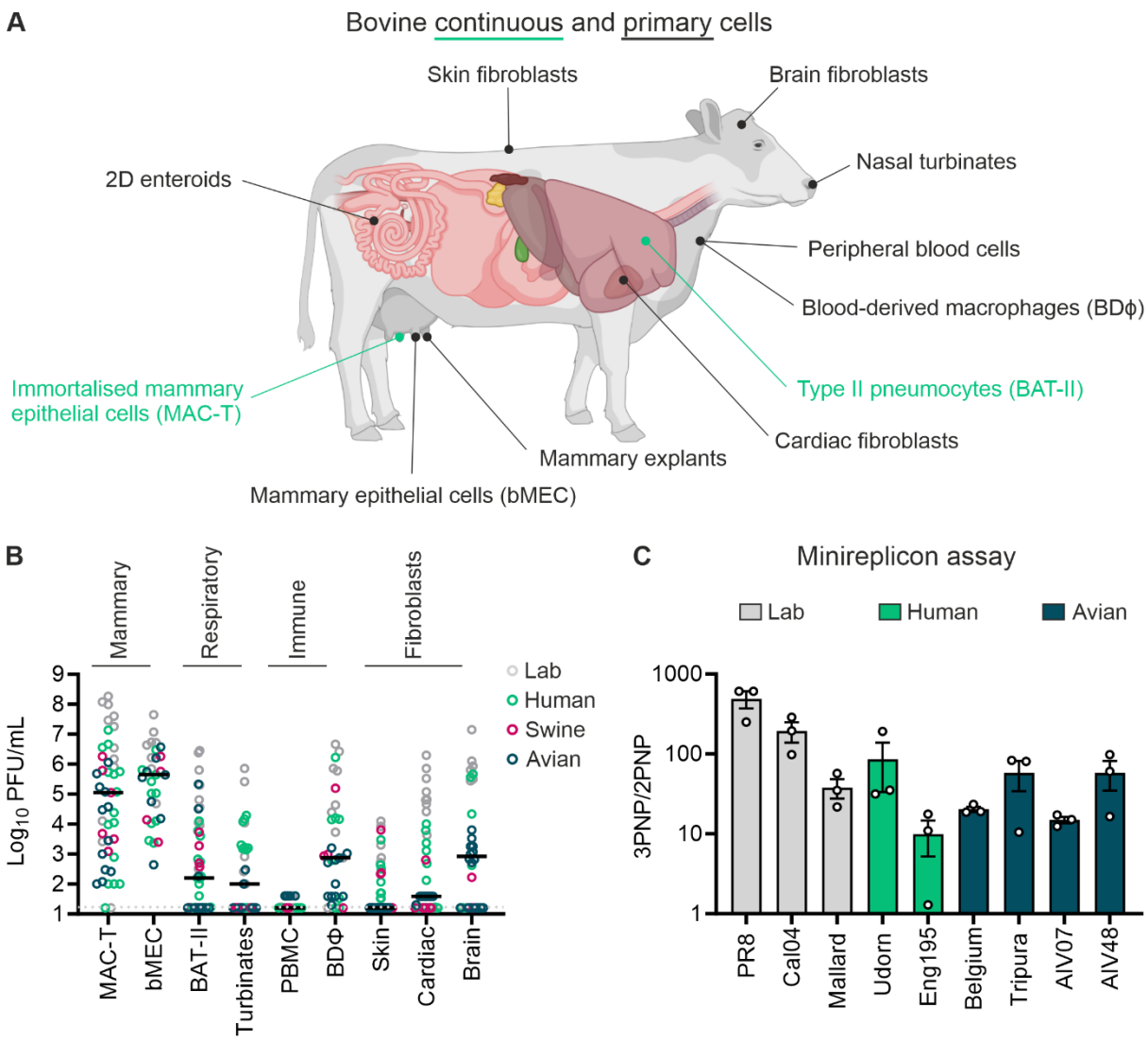

Figure 1: Cow cells are susceptible to infection with diverse IAV strains. A). Schematic representation of the anatomical source of immortalised (green) and primary (black) cells used in this study. B) The indicated cells were infected with a variety of viral strains at MOI 0.1 (bMEC) or MOI 0.01 (for the remaining cells) and virus titres measured by plaque assay at 48 hpi. Viruses were subcategorised into lab-adapted, human, swine and avian strains as indicated. Circles represent individual data points from 3 independently performed experiments, except PBMC (*n* = 1). Lines represent median. C) RNP-reconstitution assays (minireplicons) were performed in MAC-T cells by transfecting pDUAL plasmids encoding segments 1, 2, 3 and 5 from the indicated viruses alongside a firefly luciferase-expressing vRNA-like reporter plasmid. Luminescence levels were measured at 48h post transfection. Data represent mean ± SEM from three independent experiments performed in triplicate.

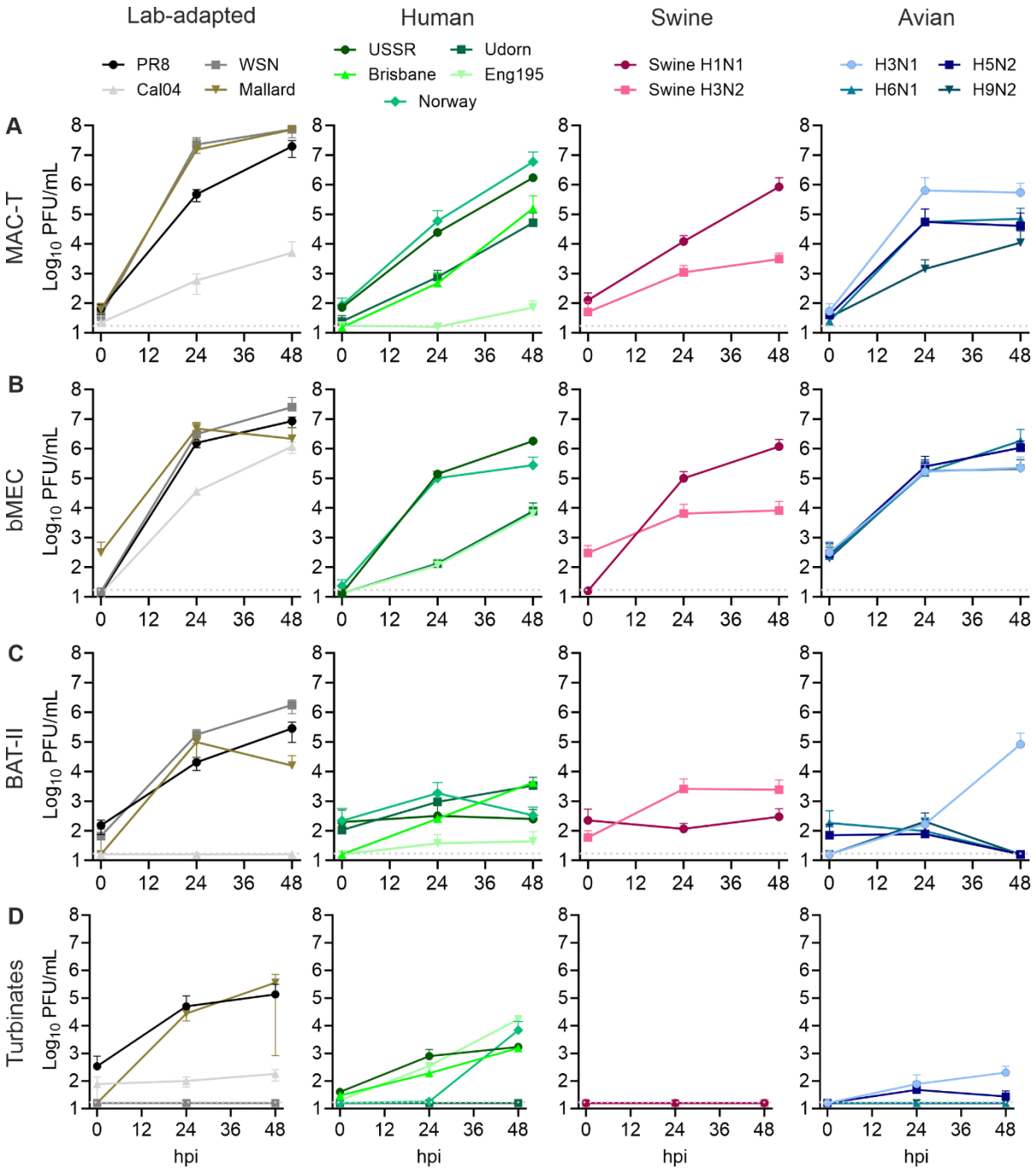

Figure S1: IAV replication kinetics in cow mammary and respiratory cells. MAC-T (A), bMEC (B), BAT-II (C) and nasal turbinates (D) were infected with the indicated viruses at MOI 0.1 (for bMEC) or 0.01 (for the remaining cells) and supernatants were collected at 0, 24 and 48 hpi. Viral titres were determined by plaque assay. Data represent mean ± SEM from three independent experiments each performed in duplicate.

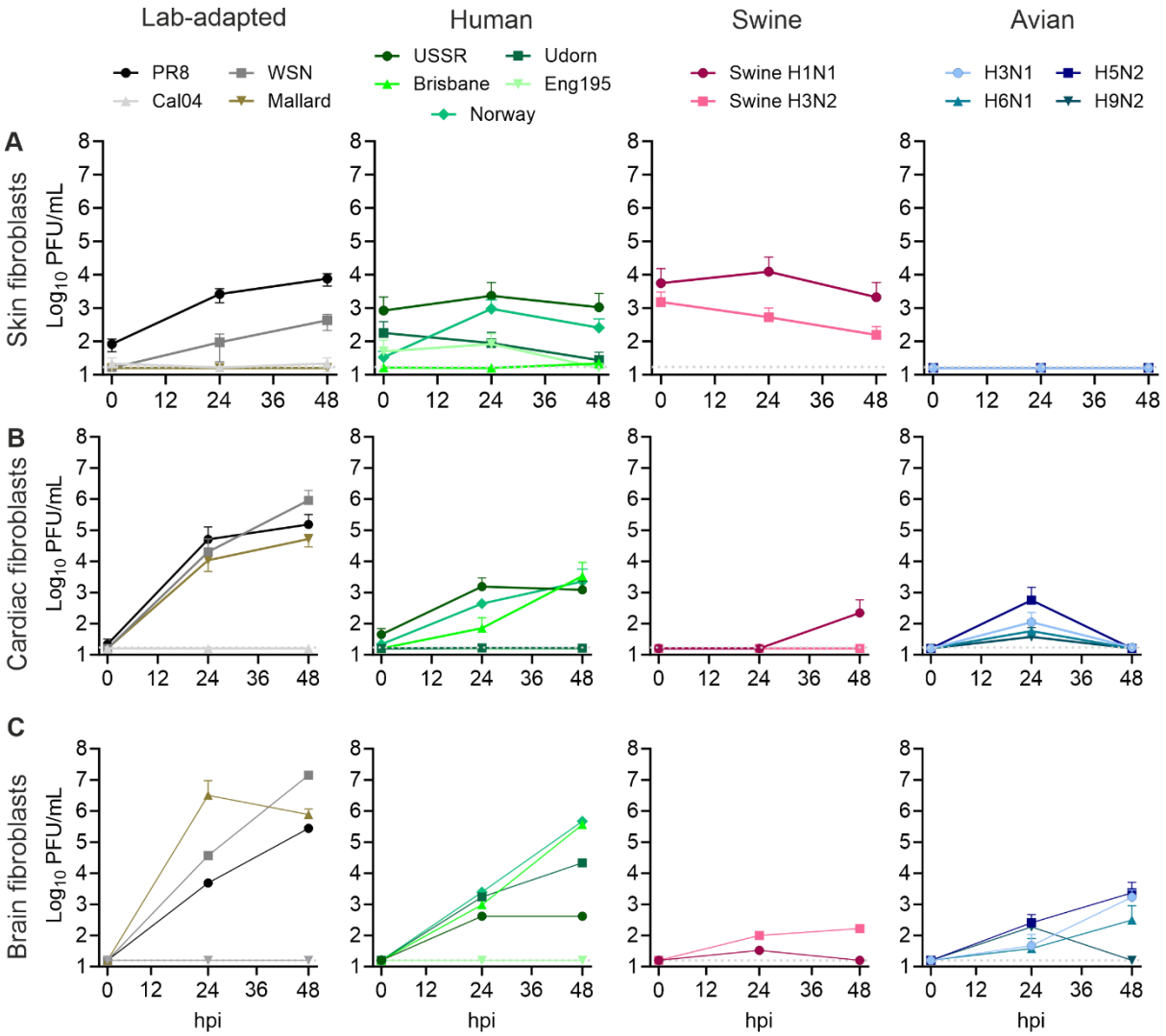

Figure S2: IAV replication kinetics in cow fibroblasts. Skin (A), cardiac (B) and brain (C) primary fibroblasts were infected with the indicated viruses at MOI 0.01 and supernatants were collected at 0, 24 and 48 hpi. Viral titres were determined by plaque assay. Data represent mean ± SEM from three independent experiments each performed in duplicate.

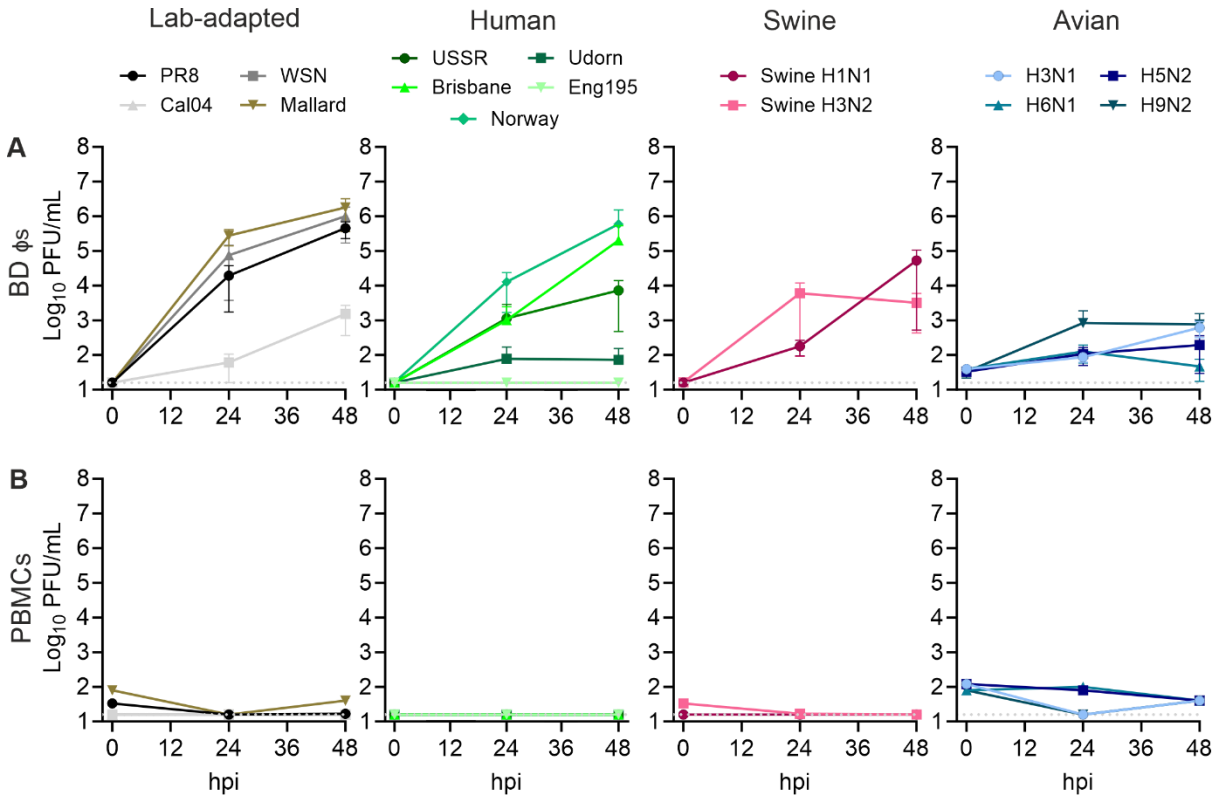

Figure S3: IAV replication kinetics in immune cells. Blood-derived macrophages (BDφ) (A) or peripheral blood mononuclear cells (PBMC) (B) were infected with the indicated viruses at MOI 0.01 and supernatants were collected at 0, 24 and 48 hpi. Viral titres were determined by plaque assay. Data represent mean ± SEM from three independent (BDφs) or a single (PBMCs) experiments each performed in duplicate.

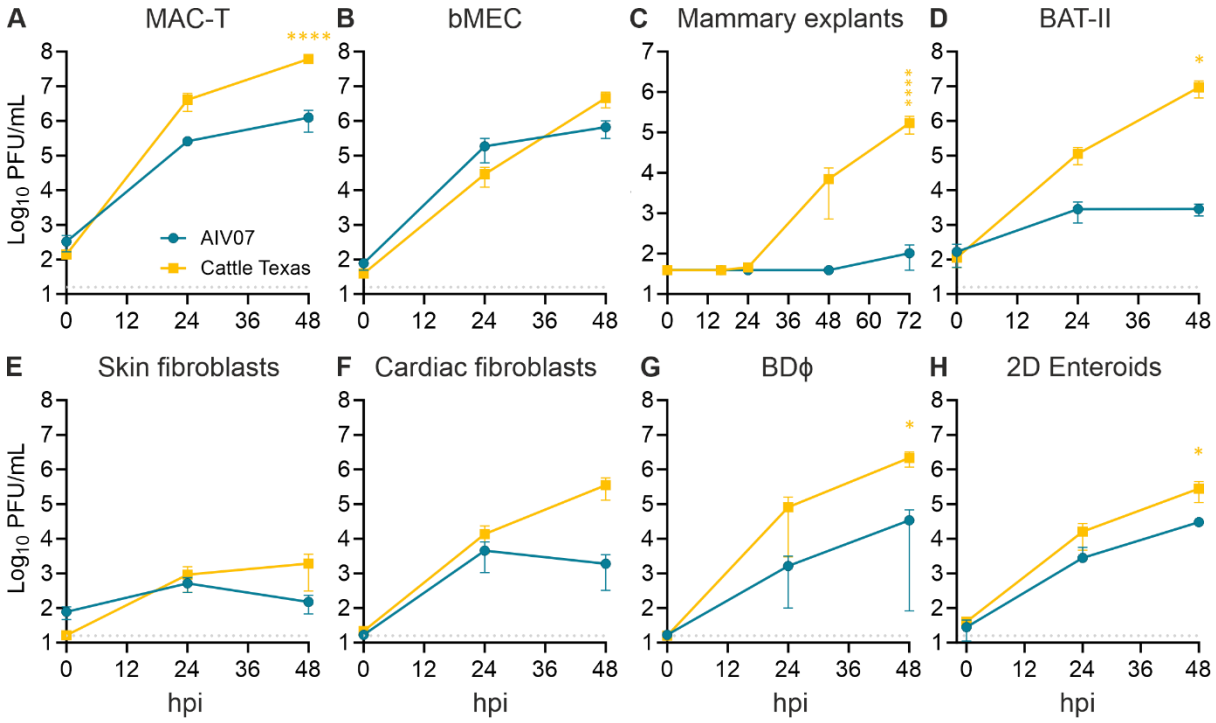

Figure 2: Cattle Texas is fitter in cow cells than an avian EURL genotype EA-2020-C precursor. The indicated cow cell systems were infected with 2:6 reassortant viruses with PR8 glycoproteins and internal gene constellations of either AIV07 (blue) or Cattle Texas (yellow) (MOI 0.1 in B, 5000 PFU/explant in C and MOI 0.01 for all other systems). Supernatants were collected at the indicated times post infection and virus titres determined by plaque assay. Data represent mean ± SEM from two/three independent experiments each performed in duplicate. Statistical annotations represent the results of unpaired t-tests performed for each individual time post infection. Cell types were immortalised mammary epithelial (MAC-T; A), primary mammary epithelial (bMEC; B), mammary gland explant (C), immortalised pneumocytes (BAT-II; D), skin fibroblast (E), cardiac fibroblast (F), blood derived macrophage (BD Φ), and enteroids (H).

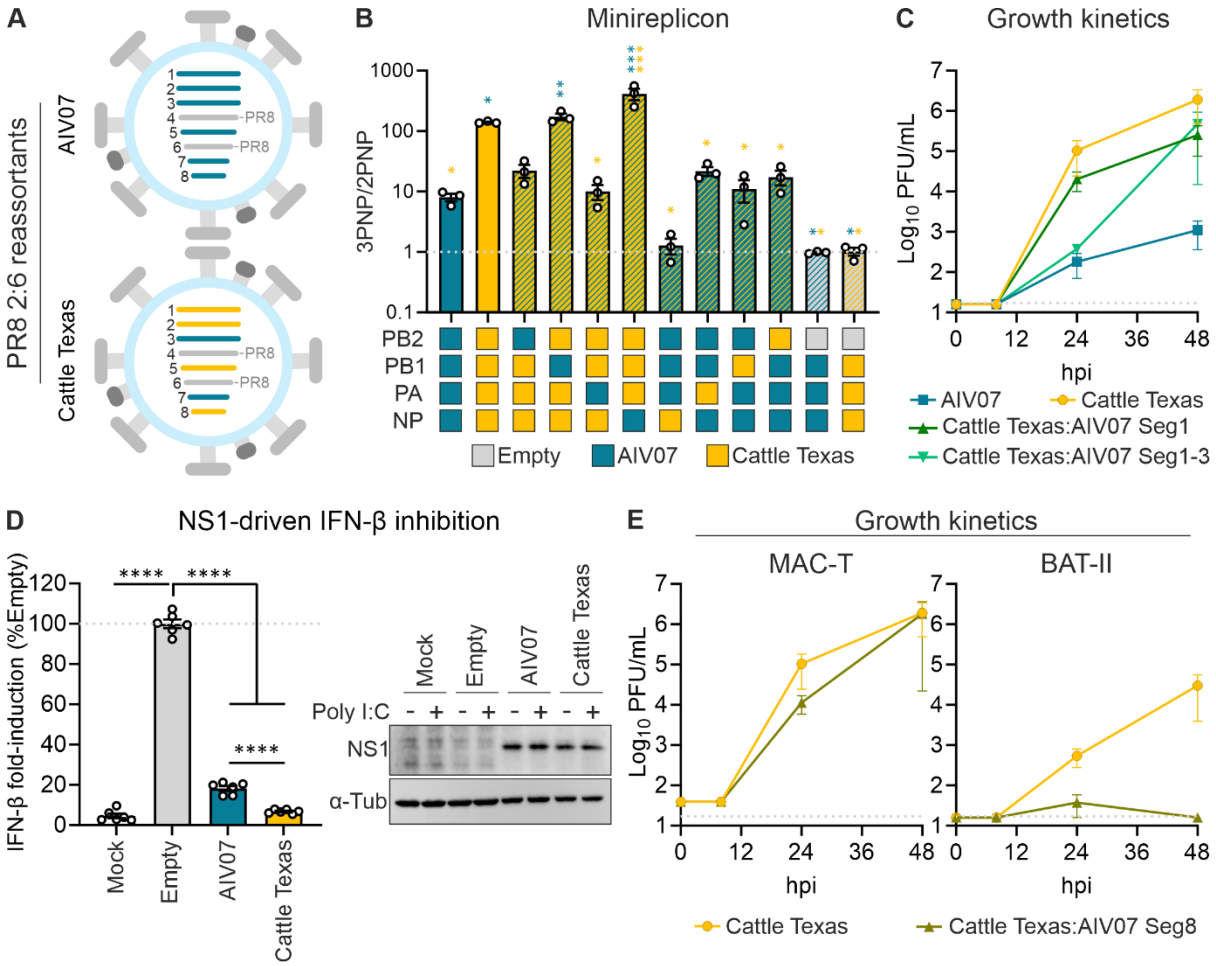

Figure 3: Increased fitness of Cattle Texas in cow cells correlates with enhanced viral polymerase activity and better NS1-driven inhibition of type I IFN induction. (A). Schematic representation of AIV07 and Cattle Texas segment origins. Blue and yellow represent European and North American ancestry, respectively. (B). RNP-reconstitution assays (minireplicons) were performed in MAC-T cells by transfecting pDUAL plasmids encoding segments 1, 2, 3 and 5 from AIV07 and Cattle Texas in the indicated combinations alongside a firefly luciferase-expressing vRNA-like reporter plasmid. Luminescence levels were measured at 48h post transfection. Data represent mean ± SEM from three independent experiments each performed in triplicate. Statistical annotations are the result of one-way ANOVA analysis. Multiple comparisons were made against full AIV07 3PNP (blue asterisks) or Cattle Texas 3PNP (yellow asterisks) using a Dunnett's test (C). MAC-T cells were infected with polymerase-segment reassortment viruses at MOI 0.01. Supernatants were collected at the indicated time points and virus titres measured by plaque assay. Data represent mean ± SEM from three independent experiments each performed in technical duplicate. (D). MAC-T cells were transfected with an IFN-β firefly luciferase-coding reporter alongside AIV07 or Cattle Texas segment 8 plasmids, and poly I:C treated 24h later. Luminescence readings were acquired after a further 24h. Data (left hand panel) represent mean ± SEM from three independent experiments each performed in technical triplicate. Statistical annotations are the result of one-way ANOVA analysis followed by a multiple comparison Dunnett's test. A western blot (right hand panel) was also performed to detect NS1, using α-Tubulin as a loading control. (E). MAC-T cells were infected with segment 8 reassortant viruses at MOI 0.01. Supernatants were collected at the indicated time points and virus titres measured by plaque assay. For all shown statistical annotations: NS – non significant, *p-value <0.05, **p-value <0.01, ***p-value <0.001 and ****p-value <0.0001 .

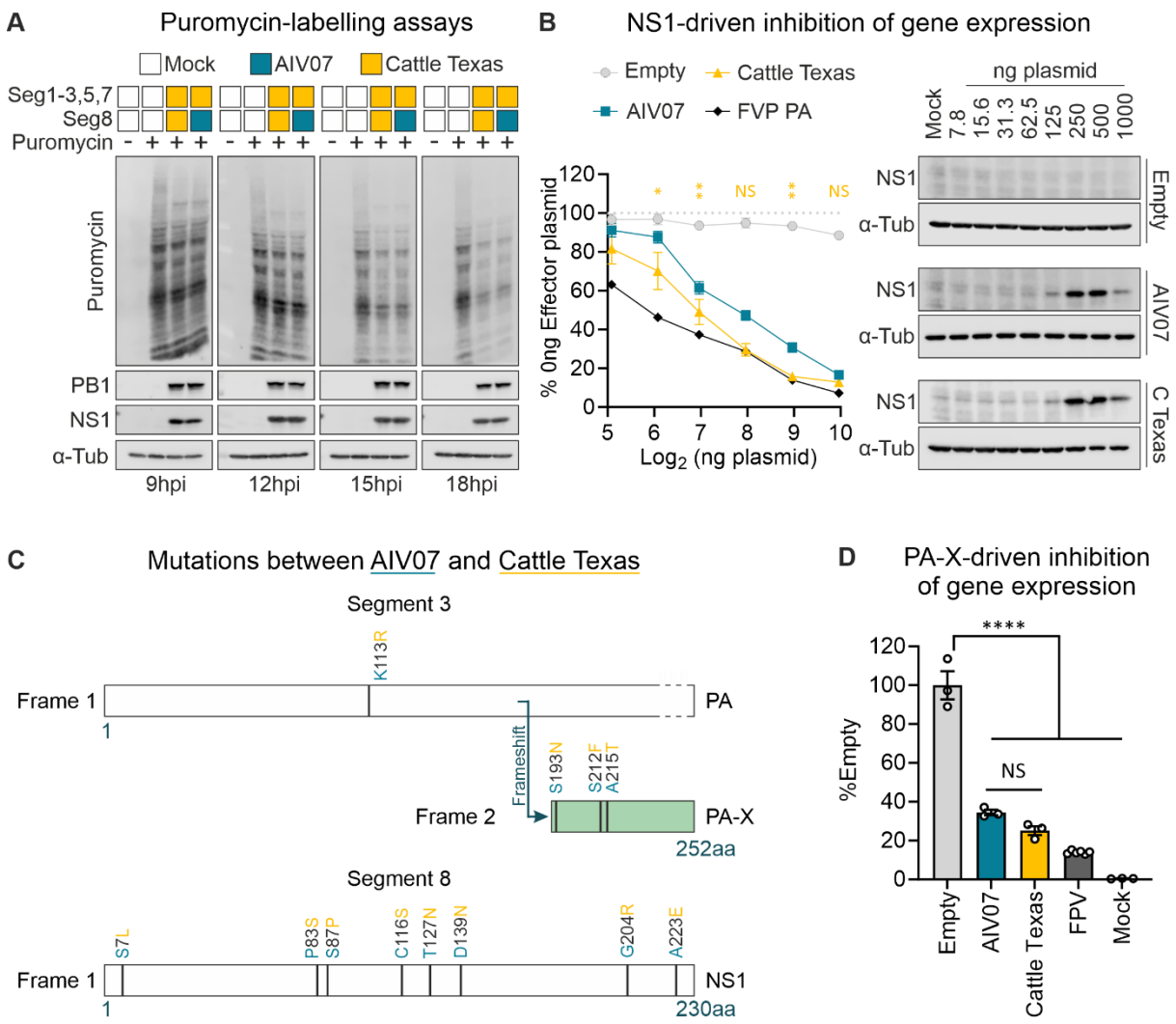

Figure S4: Cattle Texas host shutoff activity is similar to that of AIV07. (A). MAC-T cells were infected at MOI 5 and pulsed with puromycin at the indicated times post infection for 1h. Cells were lysed and new protein synthesis was measured by western blotting for puromycin. NS1 and PB1 were detected to validate infection and α-Tubulin as a loading control. (B). MAC-T cells were transfected with a reporter plasmid constitutively expressing *Renilla* luciferase under the control of a CMV promoter alongside a dose range of pDUAL plasmids expressing AIV07 or Cattle Texas NS1s. A dilution series of pDUAL plasmid expressing segment 3 of A/Chicken/Rostock/1934 H7N1 (FPV) was used as a positive control. Data represent the mean ± SEM of three independent experiments each performed in triplicate. Statistical annotations are the result of one-way ANOVA analysis performed for each plasmid dosage. Shown multiple comparisons were made between AIV07 and Cattle Texas using a Dunnett's test at given segment 8 dosages. Immunoblotting was performed to detect increasing levels of PB1 and NS1 expression, using α-Tubulin as loading control. (C) Schematic representation of PA-X and NS1 mutations between AIV07 and Cattle Texas. Open reading frames from frames 1 and 2 are represented by white and mint boxes, respectively. Amino acid differences between AIV07 (blue) and Cattle Texas in PA-X and NS1 are highlighted. (D) MAC-T cells were transfected with a reporter plasmid constitutively expressing *Renilla* luciferase under the control of a CMV promoter alongside segment 3 pDUAL plasmids (expressing PA-X). Data represent mean ± SEM from three independent experiments each performed in triplicate. Statistical annotations are the result of one-way ANOVA analysis and multiple comparisons were performed using a Dunnett's test. For (B) and (D) Luminescence readings were measured 48h post transfection.

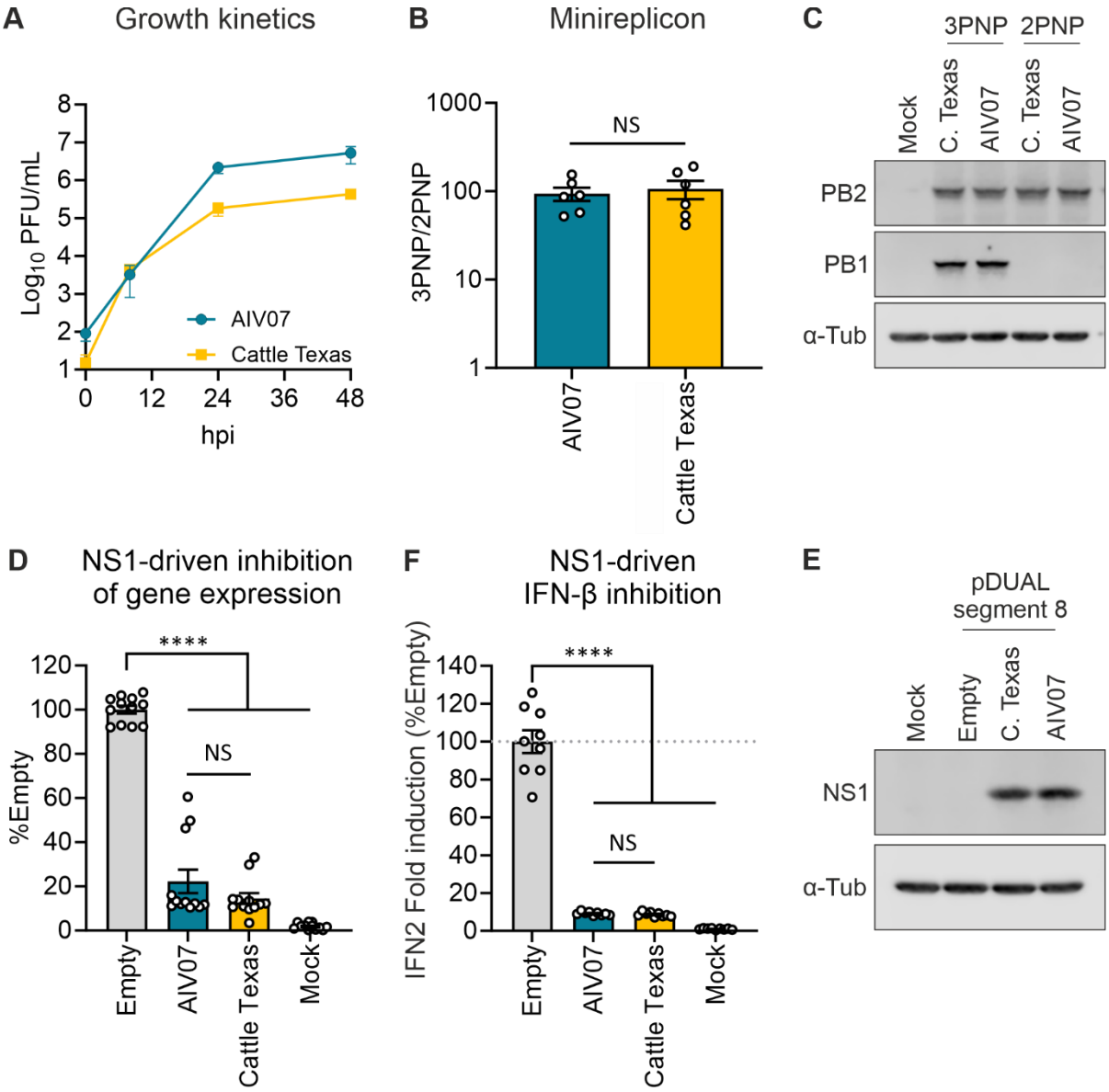

Figure S5: Cattle Texas is not fitter in chicken cells. (A) CLEC213 chicken lung epithelial cells were infected with the indicated viruses at MOI 0.01. Supernatants were collected at the indicated times post infection and virus titres were determined by plaque assay. Data represent mean ± SEM from three independent experiments each performed in duplicate. (B) CLEC213 cells were transfected with pDUAL plasmids encoding segments 1-3 and 5 of the indicated combinations of AIV07 and Cattle Texas RNP complexes alongside a firefly luciferase-expressing vRNA-like reporter plasmid. Luminescence levels were measured at 48h post transfection. Data represent mean ± SEM from three independent experiments each performed in duplicate. Statistical annotations are the result of an unpaired t-test. (C) Expression of polymerase components from (B) was examined by western blot. α-Tubulin was used as loading control. (D) CLEC213 cells were transfected with a reporter plasmid constitutively expressing *Renilla* luciferase under the control of a CMV promoter alongside AIV07 or Cattle Texas segment 8 or empty vector plasmids and luminescence readings measured 48h later. Data represent mean ± SEM from four independent experiments each performed in triplicate. Statistical annotations are the result of one-way ANOVA analysis. (E) CLEC213 cells were transfected with a chicken IFN2 promoter-driven firefly luciferase reporter alongside AIV07 or Cattle Texas segment 8 plasmids, and poly I:C treated 24h later. Luminescence readings were acquired after a further 24h. Data represent mean ± SEM from three independent experiments each performed in duplicate. Statistical annotations

are the result of one-way ANOVA analysis. (F) NS1 expression from (A) and (B) was tested by western blot. α-Tubulin was used as loading control. For D and F, multiple comparisons were performed using a Dunnett's test. For all shown statistical annotations: NS – non significant and ****p-value <0.0001 .

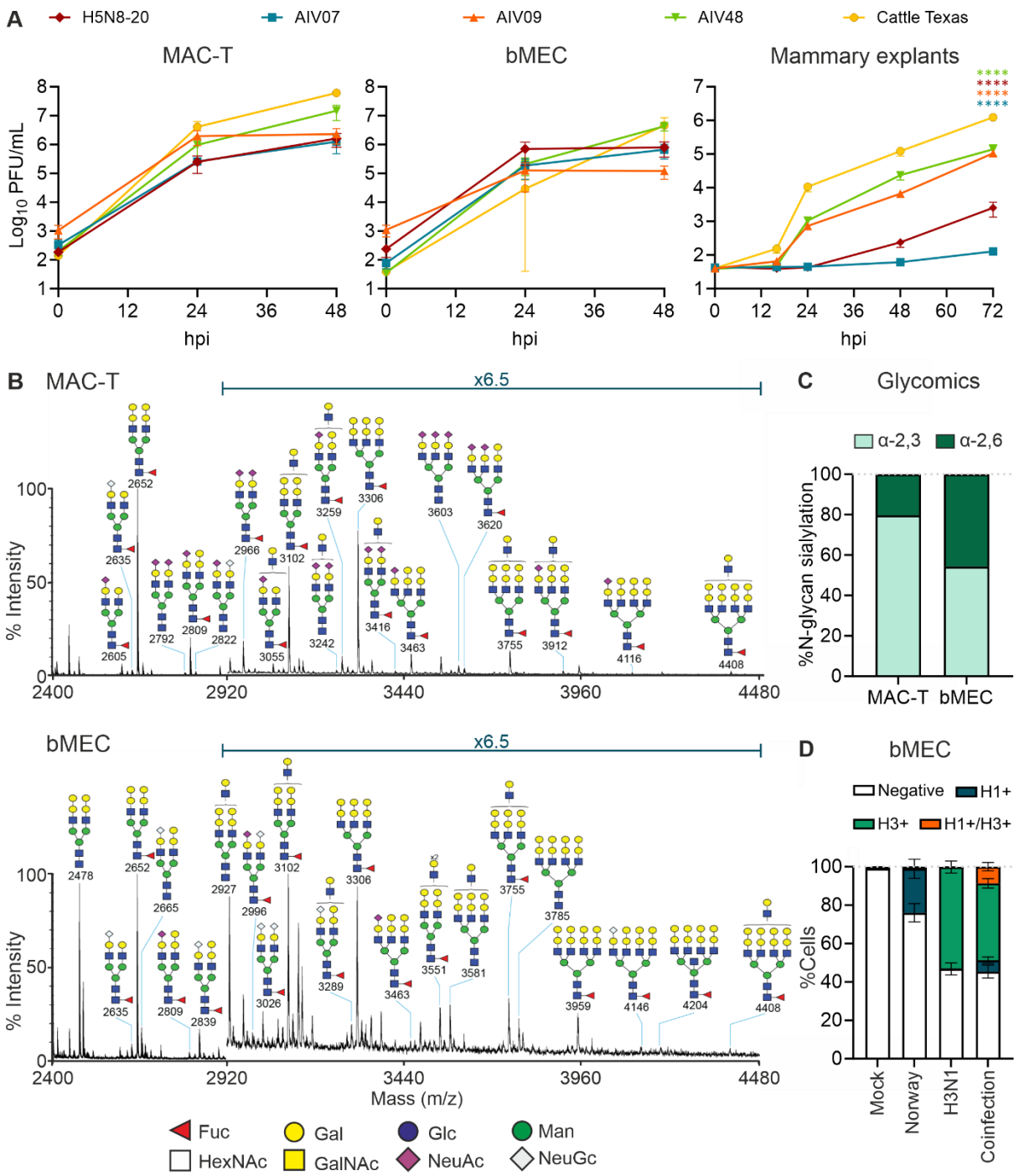

Figure 4: Cow mammary cells are infectable with viruses of human and avian origin. (A) MAC-T (MOI 0.01), bMEC (MOI 0.1) cells and mammary explants (5000 PFU/explant) were infected with the indicated PR8 2:6 viruses. Supernatants were collected at the indicated times post infection and virus titres determined by plaque assay. Statistical analysis was performed by a 2-way ANOVA and multiple comparisons were performed against Cattle Texas in specific time points using a Dunnett's test. (B) Annotated MALDI-TOF spectra of permethylated N-glycans from MAC-T and bMEC cells. Annotations show $[M + Na]^+$ molecular ions. Peak annotation is based on composition, biosynthetic knowledge and MS/MS analysis. (C) Proportions of α-2,3 and α-2,6 linked sialic acid in MAC-T and bMEC N-glycans.

909 (D) MAC-T cells were infected with combinations of Norway 2018 (pH1N1) and/or Belgium H3N1 at
910 MOI 5 for 16h. Cells were fixed, stained with anti-H1 and H3 before quantification was performed by
911 FACS analysis. Data represent mean ± SEM from three independent experiments each performed in
912 technical duplicate. For all shown statistical annotations: ****p-value <0.0001.

913

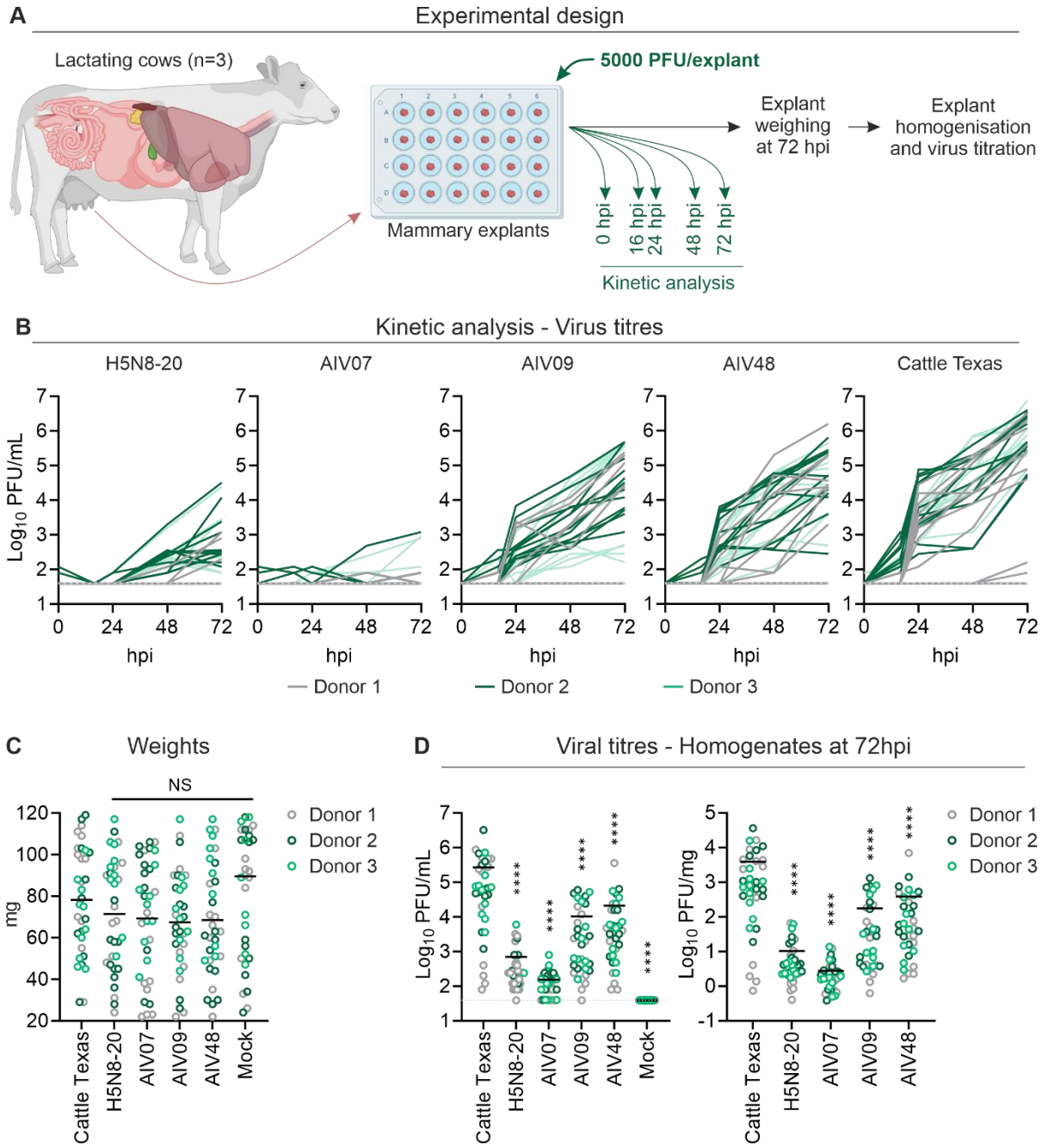

Figure S6: Infections in bovine mammary explants. (A). Schematic representation of the experimental design. (B). Multiple explants were extracted from the mammary glands from 3 donors and infected with 5000 PFU/explant. Supernatants were collected at the indicated times post infection and virus titres determined by plaque assay. Data are from individual explants coloured by donor: donor 1 (n=12), donor 2 (n=12), donor 3 (n=10). (C). Weights of explants at 72 hpi. (D). Explants were homogenised, viral titres measured by plaque assay (left panel) and normalised to individual explant weights (right panel). For C-D, black lines indicate means, circles indicate data for individual explants colour-coded by donor. Statistical annotations are the result of a one-way ANOVA test. Statistical comparisons are given against Cattle Texas using a Dunnet's test.

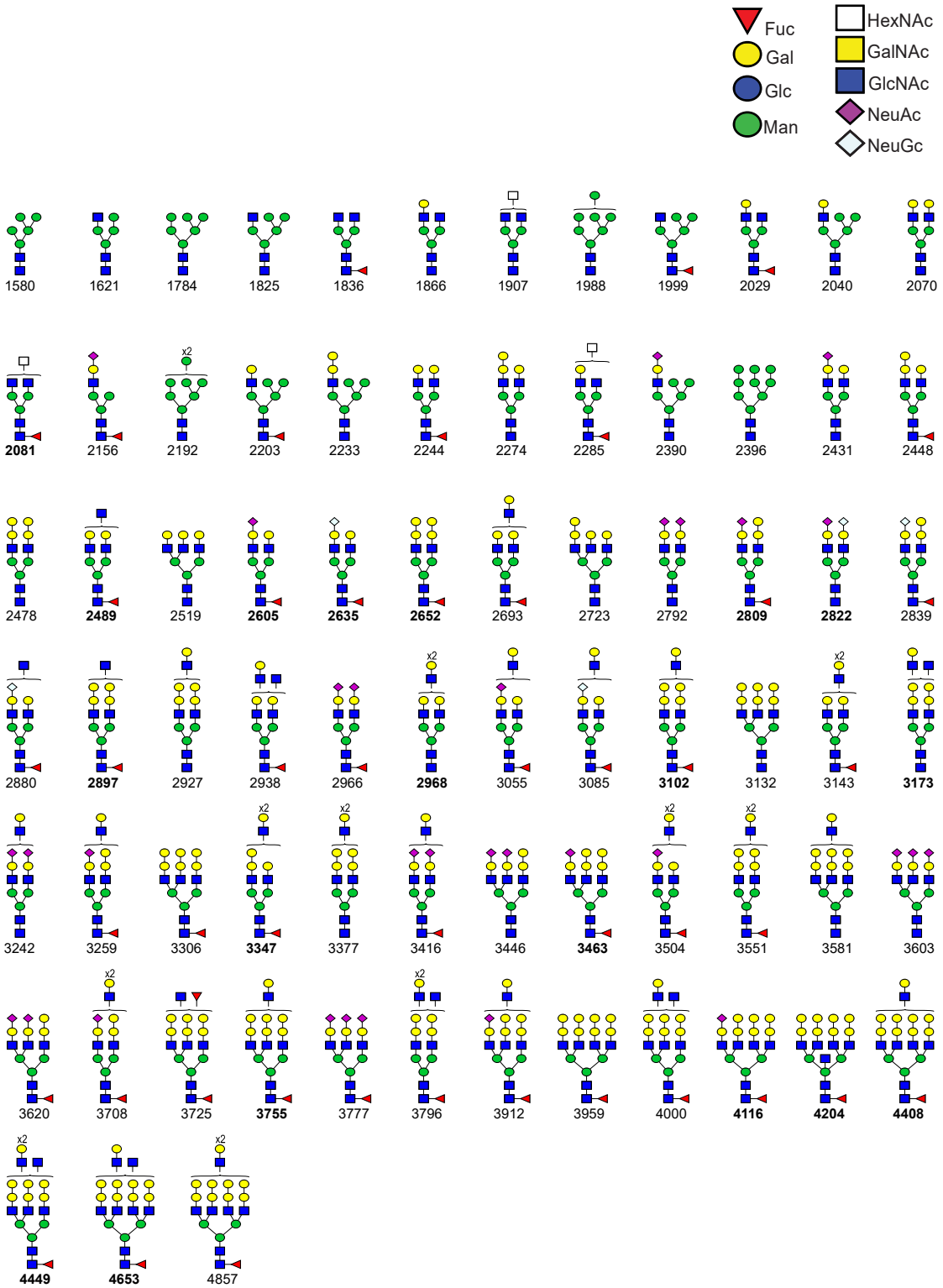

Figure S7: Structures of N-glycans from MAC-T cells. Proposed structures of the N-glycans from MAC-T cells. Structures were based on composition, biosynthetic knowledge and MS/MS analysis. Structures in bold have been confirmed directly by MS/MS. Structures were drawn according to the Symbol Nomenclature for Glycans (SNFG) guidelines.

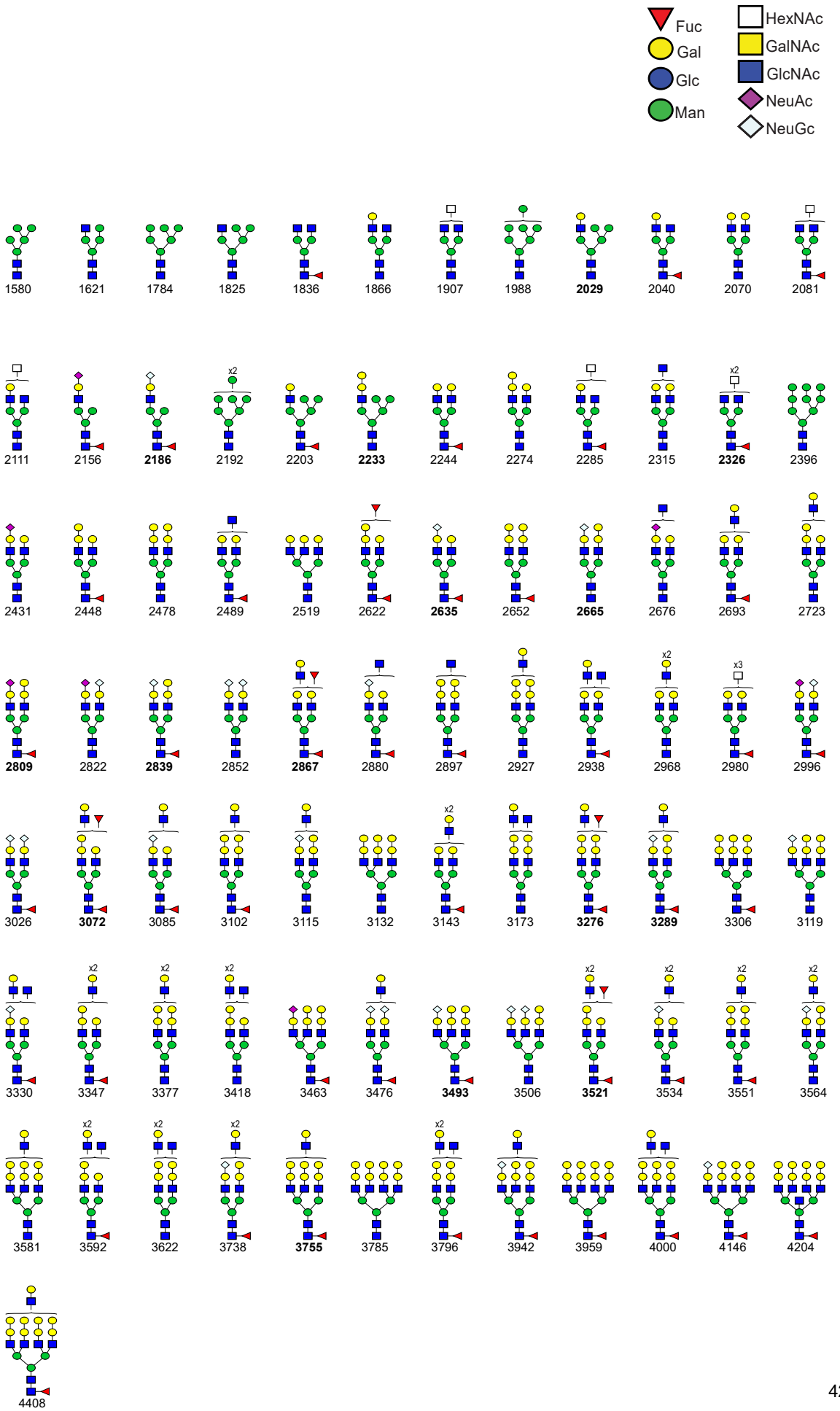
Fuc
Gal
Glc
Man
HexNAc
GalNAc
GlcNAc
NeuAc
NeuGc
1580
1621
1784
1825
1836
1866
1907
1988
2029
2040
2070
2081
2111
2156
2186
x2
2192
2203
2233
2244
2274
2285
2315
2326
x2
2396
2431
2448
2478
2489
2519
2622
2635
2652
2665
2676
2693
2723
2809
2822
2839
2852
2867
2880
2897
2927
2938
x2
2968
x3
2980
2996
3026
3072
3085
3102
3115
3132
x2
3143
3173
3276
3289
3306
3119
3330
x2
3347
x2
3377
x2
3418
3463
3476
3493
3506
x2
3521
x2
3534
x2
3551
x2
3564
3581
x2
3592
x2
3622
x2
3738
3755
3785
x2
3796
3942
3959
4000
4146
4204
4408

931

932 **Figure S8: Structures of N-glycans from bMEC cells.** Proposed structures of the N-glycans from bMEC
933 cells. Structures were based on composition, biosynthetic knowledge and MS/MS analysis. Structures
934 in bold have been confirmed directly by MS/MS. Structures were drawn according to the Symbol
935 Nomenclature for Glycans (SNFG) guidelines.
936

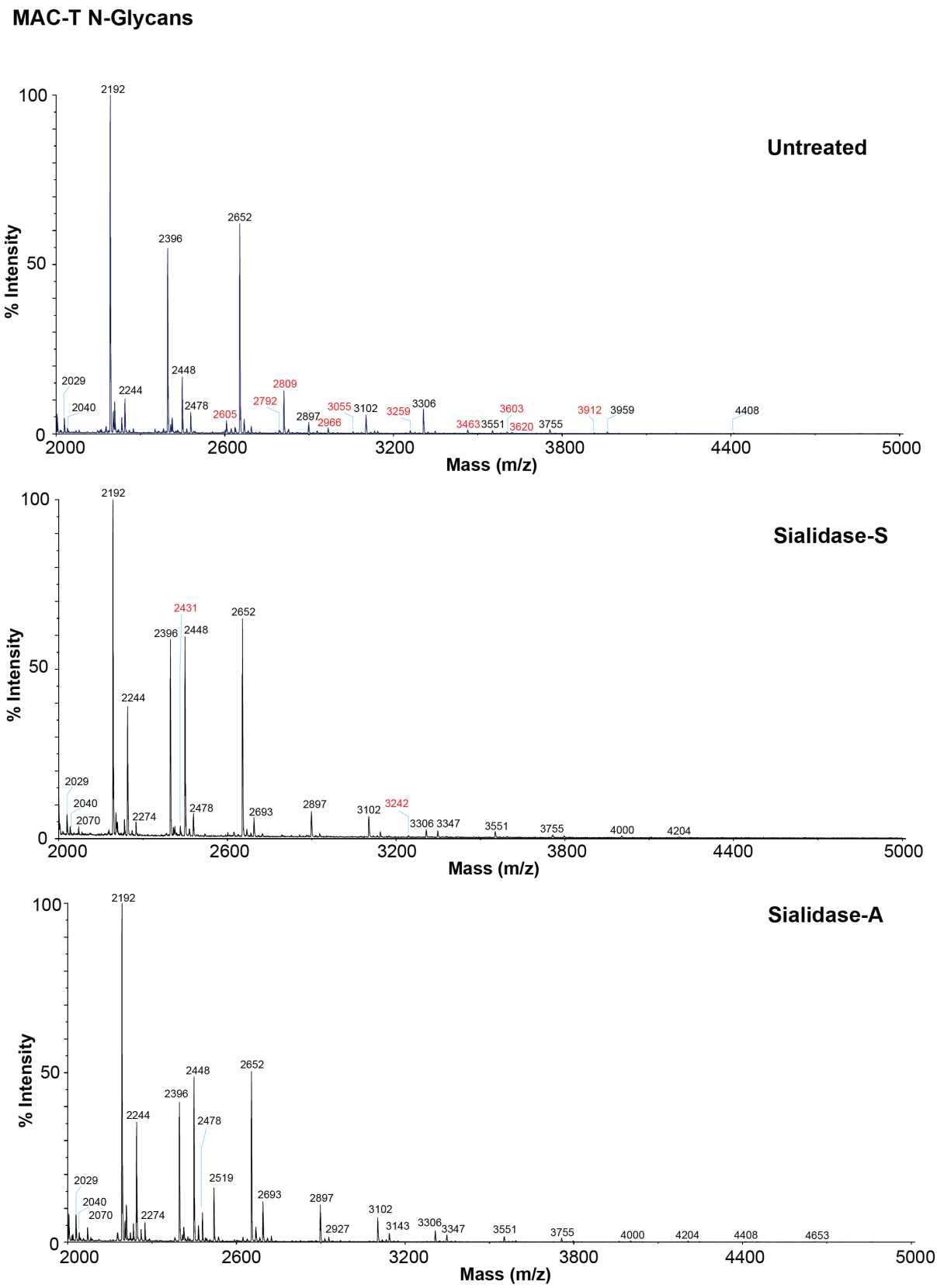

Figure S9: MALDI-TOF spectra of permethylated N-glycans from MAC-T cells following sialidase digestion. MALDI-TOF spectra of permethylated N-glycans from MAC-T cells treated with sialidase-S or sialidase-A. Annotations show $[M + Na]^+$ molecular ions and include major structures which were unsialylated (black) and sialylated (red).

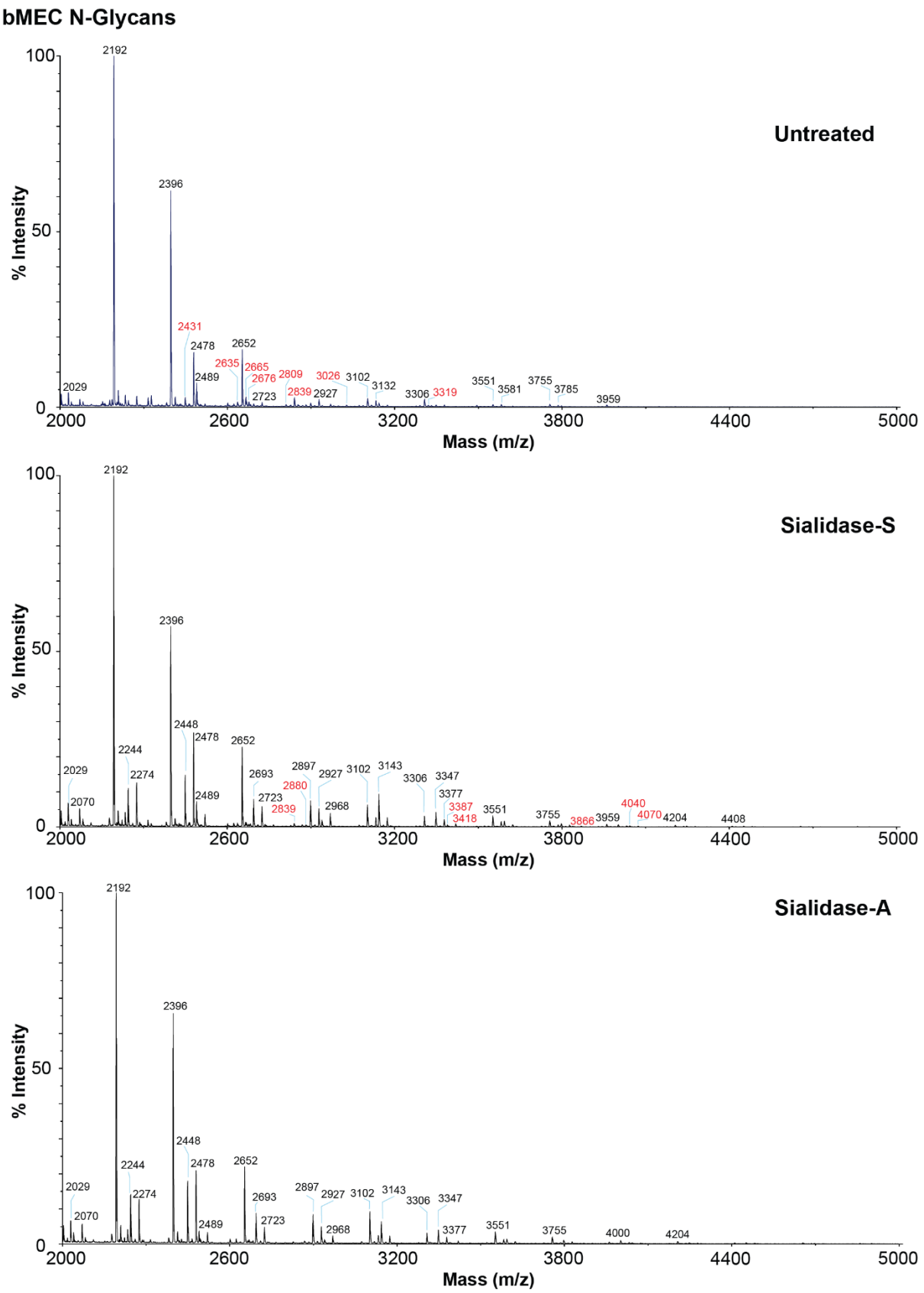

942

943 **Figure S10: MALDI-TOF spectra of permethylated N-glycans from bMEC cells following sialidase**
944 **digestion.** MALDI-TOF spectra of permethylated N-glycans from MAC-T cells treated with sialidase-S

945 or sialidase-A. Annotations show $[M + Na]^+$ molecular ions and include major structures which were
946 unsialylated (black) and sialylated (red).

947